

# Phonon Hall Viscosity in Magnetic Insulators

Mengxing Ye,<sup>1</sup> Lucile Savary,<sup>2</sup> and Leon Balents<sup>1</sup>

<sup>1</sup>*Kavli Institute for Theoretical Physics, University of California, Santa Barbara, CA 93106, USA*

<sup>2</sup>*Université de Lyon, École Normale Supérieure de Lyon, Université Claude Bernard Lyon I, CNRS, Laboratoire de physique, 46, allée d'Italie, 69007 Lyon, France*

(Dated: December 29, 2021)

The Phonon Hall Viscosity is the leading term evincing time-reversal symmetry breaking in the low energy description of lattice phonons. It may generate phonon Berry curvature, and can be observed experimentally through the acoustic Faraday effect and thermal Hall transport. We present a systematic procedure to obtain the phonon Hall viscosity induced by phonon-magnon interactions in magnetic insulators under an external magnetic field. We obtain a general symmetry criterion that leads to non-zero Faraday rotation and Hall conductivity, and clarify the interplay between lattice symmetry, spin-orbit-coupling, external magnetic field and magnetic ordering. The symmetry analysis is verified through a microscopic calculation. By constructing the general symmetry-allowed effective action that describes the spin dynamics and spin-lattice coupling, and then integrating out the spin fluctuations, the leading order time-reversal breaking term in the phonon effective action, i.e. the phonon Hall viscosity, can be obtained. The analysis of the square lattice antiferromagnet for a cuprate Mott insulator,  $\text{Sr}_2\text{CuO}_2\text{Cl}_2$ , is presented explicitly, and the procedure described here can be readily generalized to other magnetic insulators.

*Introduction.*— In a material without time-reversal symmetry, the elastic stress may contain a non-dissipative term proportional to the time derivative of the elastic strain, the coefficient of which defines the phonon Hall viscosity (PHV) [1–3]. The PHV is analogous to the Hall viscosity in a fluid, which has been heavily studied in quantum Hall states [4–7], and superconductors/superfluids[6–8]. The PHV can be represented as a momentum space gauge field for phonons, and as such encodes the Berry curvature of phonon eigenstates. Multiple mechanisms can generate a PHV [9–14], including subtle band effects [15]. In this paper, we consider the PHV generated by the magnetoelastic coupling of strain and spins [9, 14], taking into account exchange and the Zeeman interaction of the spins with an external magnetic field.

The phonon Hall viscosity may be probed in experiments such as acoustic Faraday rotation and thermal Hall transport. The first is a measure of broken degeneracy between right and left circularly polarized acoustic phonons; the Faraday rotation angle is proportional to the PHV [2, 9, 16]. The second describes a transverse heat current in response to a thermal gradient, and the part of such heat current carried by phonons – the phonon Hall effect – is proportional to the PHV (in the ballistic phonon regime). Recent thermal Hall measurements in cuprate compounds [17–19] suggest that the phonon Hall effect may dominate the thermal Hall signal in both the Mott insulating and pseudogap phases of cuprates.

In this paper, we present a systematic procedure to obtain the PHV in magnetic insulators, based on the coupling of spins to elastic strains. We concentrate mainly on the PHV terms that contribute to the acoustic Faraday rotation and phonon Hall conductivity. We first intro-

duce the effective field theory and the expression for the viscosity coefficients. We follow with a thorough symmetry analysis in different phases and regimes, arriving at a symmetry criterion for a nonzero PHV, which we verify through a microscopic calculation. We conclude with a discussion of experimental implications, spin-orbit coupling, and open questions.

*Phonon effective action and magnetoelastic coupling*— The PHV term in the effective linear response action is [1, 5],

$$\mathcal{S}_{\text{PHV}} = \frac{1}{2} \sum_{\mathbf{q}, \Gamma, \Gamma'} \int dt \eta_{\Gamma\Gamma'}^H(\mathbf{q}) (\mathcal{E}_{\Gamma, \mathbf{q}} \dot{\mathcal{E}}_{\Gamma', -\mathbf{q}} - \dot{\mathcal{E}}_{\Gamma, \mathbf{q}} \mathcal{E}_{\Gamma', -\mathbf{q}}), \quad (1)$$

where  $\mathcal{E}_{ij} = \frac{1}{2}(\partial_i u_j + \partial_j u_i)$  is the strain tensor,  $i, j$  label Euclidean coordinates, and  $\mathbf{u}$  is the lattice displacement field. Here  $\dot{\mathcal{E}} = \partial_t \mathcal{E}$ , and  $\Gamma, \Gamma'$  are the irreducible representations (irreps) of a group whose precise definition we make clear below. The Hall viscosity  $\eta_{\Gamma\Gamma'}^H(\mathbf{q})$  describes the stress  $\Sigma_\Gamma$  resulting from a time-dependent strain  $\mathcal{E}_{\Gamma'}$ , i.e.  $\Sigma_\Gamma \sim \delta \mathcal{S}_{\text{PHV}} / \delta \mathcal{E}_{\Gamma'} \sim \eta_{\Gamma\Gamma'}^H \dot{\mathcal{E}}_{\Gamma'}$  [7]. As we will discuss at length below, symmetry constrains greatly which  $\Gamma\Gamma'$  lead to a nonvanishing  $\eta_{\Gamma\Gamma'}^H$ . We allow for a momentum dependence of the Hall viscosity  $\eta_{\Gamma\Gamma'}^H(\mathbf{q}) = -\eta_{\Gamma\Gamma'}^H(-\mathbf{q})$ . [20]

The Lagrangian density for the magnetoelastic coupling can be expressed as

$$\mathcal{L}_{sl} = \sum_{\Gamma, a} \lambda_{\Gamma, a} \mathcal{E}_\Gamma(\mathbf{x}, \tau) \cdot \mathcal{O}_{\Gamma, a}(\mathbf{x}, \tau), \quad (2)$$

where  $\lambda_{\Gamma, a}$  denotes the magnetoelastic coupling strength in units of energy to the  $\Gamma$ th component of the strain field  $\mathcal{E}_\Gamma$  of (each independent copy  $a$  of) the spin operator composite  $\mathcal{O}_{\Gamma, a}(\mathbf{x}, \tau)$  which transforms under the same  $\Gamma$  irrep.

The Hall viscosity itself is then obtained by extracting terms linear in the phonon energy  $\omega$  (reflecting the fact that the PHV is time-reversal odd). More precisely, the Hall viscosity “coefficient”  $\eta_{\Gamma\Gamma'}^H$  is obtained from the correlation of  $\mathcal{O}_\Gamma$ ,  $\mathcal{O}_{\Gamma'}$  as [14]:

$$\frac{i\eta_{\Gamma\Gamma'}^H(\mathbf{q})}{\lambda_\Gamma\lambda_{\Gamma'}} = \lim_{\omega \rightarrow 0} \partial_\omega \sum_{a,a'} \langle \mathcal{O}_{\Gamma a}(-\mathbf{q}, \tau) \cdot \mathcal{O}_{\Gamma' a'}(\mathbf{q}, 0) \rangle_{-i\omega+0+}, \quad (3)$$

where  $\langle \mathcal{A} \rangle_{\omega_n} \equiv \int_0^\beta d\tau e^{i\omega_n \tau} \langle T_\tau \mathcal{A}(\tau) \rangle$  denotes the Fourier transform,  $\tau$  is imaginary time,  $\omega_n = 2\pi n/\beta$  is the  $n$ th bosonic Matsubara frequency and  $T_\tau$  denotes imaginary-time ordering.

*Magnetic system.*—We now specify the theory to calculate the correlations of the  $\mathcal{O}$  operators. We study a two-dimensional spin system which orders antiferromagnetically in zero field. Because we will compute  $\eta_{\Gamma\Gamma'}^H(\mathbf{q})$  for small momentum  $\mathbf{q}$  at low temperature (compared to the Debye temperature and magnon bandwidth), it is enough to consider low-energy spin and lattice fluctuations. We therefore employ a path integral approach, and describe the low energy dynamics in terms of continuous fields: the irrep components of the strain tensor ( $\mathcal{E}_\Gamma$ ) and the staggered ( $\mathbf{n}$ ) and uniform ( $\mathbf{m}$ ) magnetizations. The latter two fields are described by the well-known nonlinear sigma model (see SM), with the constraints  $|\mathbf{n}|^2 = 1$  and  $\mathbf{n} \cdot \mathbf{m} = 0$ .

The  $\mathcal{O}$  correlations are obtained from the nonlinear sigma model as follows. We will consider a weak applied field along the  $z$ -axis,  $\mathbf{h} = h\hat{\mathbf{z}}$ . We assume that in the zero-field limit the uniform magnetization vanishes,  $\lim_{h \rightarrow 0} \langle \mathbf{m} \rangle = 0$ , and the Néel vector  $\mathbf{n}$  lies along the  $x$ -axis,  $\lim_{h \rightarrow 0} \langle \mathbf{n} \rangle = n_0 \hat{\mathbf{x}}$ . Then constraints are solved via  $\mathbf{n} = (n_0, \mathbf{n}_\perp)$ , with  $n_0 = \sqrt{1 - \mathbf{n}_\perp^2}$ ,  $\mathbf{m} = (m_x, \mathbf{m}_\perp)$  and  $m_x = -\mathbf{n}_\perp \cdot \mathbf{m}_\perp / n_0$ . We also define  $\mathbf{m}$  through  $\mathbf{m} = \chi h \hat{\mathbf{z}} + \mathbf{m}$ , highlighting the field-induced uniform magnetization  $\chi h \hat{\mathbf{z}}$  ( $\chi$  is the magnetic susceptibility along the  $z$ -axis).  $\mathbf{n}_\perp, \mathbf{m}_\perp$  form two canonically conjugate pairs of Gaussian fields and may be considered “spin-wave variables”. We also define  $\omega_{\alpha, \mathbf{k}}$  to be the dispersion for the magnon branch  $\alpha \in \{y, z\}$ . In the case of a Heisenberg model with exchange  $J$ , plus weak anisotropies of the order of  $\Delta_\alpha$ , the dispersion relation takes the form  $\omega_{\alpha, \mathbf{k}} = v_m \sqrt{k_x^2 + k_y^2 + \delta_\alpha^2}$ , where  $v_m$  is the magnon velocity and  $\delta_\alpha$  are the magnon gaps in units of inverse length:  $\delta_y = \Delta_y/v_m$ ,  $\delta_z = \sqrt{\Delta_z^2 + h^2}/v_m$ .

From this, we find that correlators of the form  $\langle nn \rangle, \langle mm \rangle$  are even functions of frequency and given in the SM, and only the “mixed” correlators  $\langle nm \rangle$  are odd in frequency:

$$\langle n_{\alpha, \mathbf{k}} m_{\bar{\alpha}, -\mathbf{k}} \rangle_{\omega_n} = \epsilon_{x\alpha\bar{\alpha}} \frac{\omega_n a_0^2}{S} \mathcal{D}_\alpha(\mathbf{k}, \omega_n), \quad (4)$$

where  $\epsilon$  is the Levi-Civita tensor,  $\bar{\alpha} \neq \alpha, x$ ,  $a_0$  is the lattice constant of the magnetic layer, and  $\mathcal{D}_\alpha^{-1}(\mathbf{k}, \omega_n) = \omega_n^2 + \omega_{\alpha, \mathbf{k}}^2$ .

The magnetic operators  $\mathcal{O}_{\Gamma, a}$  may be expressed as polynomials in the staggered and uniform magnetizations  $\mathbf{n}, \mathbf{m}$ . In order to understand their form, we must proceed to a thorough symmetry analysis.

*Symmetry group considerations.*— We call  $G$  the lattice space group of the crystal in the paramagnetic phase. We also define  $\mathbf{G}$  to be its associated (paramagnetic) *magnetic* space group,  $\mathbf{G} = G \times \{\text{Id}, \mathcal{T}\}$ . Spontaneous ordering with staggered magnetization  $\mathbf{n}$  and/or an external field  $\mathbf{h}$  reduce the system’s symmetry to  $\mathbf{G}(\mathbf{n}, \mathbf{h})$ . For example, the subgroup of  $\mathbf{G}$  which preserves the AFM order defines the magnetic space group of the AFM,  $\mathbf{G}(\mathbf{n}, \mathbf{0})$ , and the subgroup which preserves the Zeeman interaction with the magnetic field  $\mathbf{h}$  defines the magnetic space group of the paramagnet in a field,  $\mathbf{G}(\mathbf{0}, \mathbf{h})$ . In simple cases, the magnetic space group of the AFM in an external field,  $\mathbf{G}(\mathbf{n}, \mathbf{h})$ , can be found as the intersection set of  $\mathbf{G}(\mathbf{n}, \mathbf{0})$  and  $\mathbf{G}(\mathbf{0}, \mathbf{h})$ .

Ultimately the PHV is defined in the *effective* action,  $\mathcal{S}_{\text{PHV}}$  from Eq. (1), purely in the phonon space. It results, in the framework described here, from integrating out the magnetic degrees of freedom  $\mathbf{m}, \mathbf{n}$ , i.e. from carrying out the integral in Eq. (A2) of the SM. One may then observe a simplifying feature of the *representation* of the symmetry operations on the lattice terms. In particular, *the translation operation acts as the identity on the lattice strain field*. Indeed, in  $\mathcal{L}_{sl}$ ,  $\mathcal{O}_\Gamma$  and  $\mathcal{E}_\Gamma$  are *independently* translationally invariant. As a consequence, the appropriate representation of  $\mathbf{G}(\mathbf{n}, \mathbf{h})$  acting on the terms in the effective phonon action (in the presence of AFM order and in a field) is that of the *magnetic point group*  $\mathbf{G}^{\text{eff}}(\mathbf{n}, \mathbf{h})$  obtained through the group morphism  $\Pi : (W, t) \mapsto (W, 0)$ , where  $(W, t) \in \mathbf{G}(\mathbf{n}, \mathbf{h})$  and  $W, t$ , are respectively the (anti)linear and translational parts of  $(W, t)$  and 0 denotes here the zero translation. The morphism theorem applies and

$$\mathbf{G}^{\text{eff}}(\mathbf{n}, \mathbf{h}) \cong \mathbf{G}(\mathbf{n}, \mathbf{h}) / \mathbf{T}(\mathbf{n}, \mathbf{h}), \quad (5)$$

i.e.  $\mathbf{G}^{\text{eff}}(\mathbf{n}, \mathbf{h})$  is isomorphic to the factor group  $\mathbf{G}(\mathbf{n}, \mathbf{h}) / \mathbf{T}(\mathbf{n}, \mathbf{h})$ , where  $\mathbf{T}(\mathbf{n}, \mathbf{h})$  is the pure translation subgroup of  $\mathbf{G}(\mathbf{n}, \mathbf{h})$ . The group  $\mathbf{G}^{\text{eff}}(\mathbf{n}, \mathbf{h})$  may now be used to analyze the PHV. In particular, distinct irreps  $\Gamma, \Gamma'$  under  $\mathbf{G}$  may collapse to the same irrep under  $\mathbf{G}^{\text{eff}}(\mathbf{n}, \mathbf{h})$ , allowing the corresponding strain components  $\mathcal{E}_\Gamma, \mathcal{E}_{\Gamma'}$  to couple in the PHV term.

*Application.*— As an example, we now consider a 3D crystal composed of finite thickness regions whose symmetry is given by the *layer group*  $G = P4/mmm$  (layer group number 61, see e.g. Ref. [21]), whose point group is  $D_{4h}$  in the sense that  $G$  is the semi-direct product of the point group  $4/mmm$  ( $D_{4h}$ ) and the 2D translation group  $P$  of a square Bravais lattice. The layer group is the natural framework to describe those properties of quasi-2d solids which are independent of the stacking structure (however, some stackings may reduce the point group symmetries, and thereby relax restrictions on

	zero field	$\mathbf{h} = h\hat{\mathbf{z}}$	
		lattice and spin	lattice effective
paramagnet	$G = P4/mmm1'$	$G(\mathbf{0}, h\hat{\mathbf{z}}) = P4/mm'm'$	$G^{\text{eff}}(\mathbf{0}, h\hat{\mathbf{z}}) = 4/mm'm'$
high sym. AFM	$G(\hat{\mathbf{x}}, \mathbf{0}) = \langle i, \mathcal{TX}, \mathcal{TY}, C_{2x}, \mathcal{TC}_{2z} \rangle$	$G(\hat{\mathbf{x}}, h\hat{\mathbf{z}}) = \langle i, XY, \mathcal{TC}_{2y}, XC_{2z} \rangle$	$G^{\text{eff}}(\hat{\mathbf{x}}, h\hat{\mathbf{z}}) = \langle i, \mathcal{TC}_{2y}, C_{2z} \rangle$
low sym. AFM	$G(\hat{\mathbf{e}}, \mathbf{0}) = \langle i, \mathcal{TX}, \mathcal{TY}, \mathcal{TC}_{2z} \rangle$	$G(\hat{\mathbf{e}}, h\hat{\mathbf{z}}) = \langle i, XY, XC_{2z} \rangle$	$G^{\text{eff}}(\hat{\mathbf{e}}, h\hat{\mathbf{z}}) = \langle i, C_{2z} \rangle$

TABLE I. Summary of the magnetic groups (in the Hermann-Mauguin notation) for crystallographic layer group  $G = P4/mmm$ . Rows denote different values for  $\mathbf{n}$ : without magnetic order, and for the two distinct orientations of the staggered magnetization in the  $xy$  plane (here  $\hat{\mathbf{e}}$  is a generic vector *not* along a high-symmetry axis in the plane), and columns specify the zero and finite field cases, and the effective magnetic group for the effective lattice theory. Here  $i$  is inversion,  $P4/mmm1' = P4/mmm \times (\text{Id} + \mathcal{T})$  is a grey group,  $P4/mm'm' = (C_{4h} + \mathcal{T} \times (D_{4h} - C_{4h})) \times P$  is a black-white group in which  $m'$  denotes the vertical mirror composed with  $\mathcal{T}$ . The symbol  $\langle \cdot \rangle$  indicates the group generated by the “.” operations.

the PHV). The cuprate Mott insulator  $\text{Sr}_2\text{CuO}_2\text{Cl}_2$  with space group  $I4/mmm$  (number 139) is such an example. The translation group  $P$  is generated by translations  $X, Y$  within the  $xy$  plane, i.e. by the Bravais lattice vectors  $\hat{\mathbf{x}}, \hat{\mathbf{y}}$ , respectively. To characterize the lattice strain field, only the *point* group is relevant, and the decomposition of the strain tensor  $\mathcal{E}$  into irreducible representations (irreps) of  $D_{4h}$  reads:

$$\begin{aligned} \mathcal{E}_{A_1} &= \mathcal{E}_{xx} + \mathcal{E}_{yy}, \mathcal{E}_{B_1} = \mathcal{E}_{xx} - \mathcal{E}_{yy}, \mathcal{E}_{B_2} = \mathcal{E}_{xy}, \\ \mathcal{E}_E &= \{\mathcal{E}_{Ex}, \mathcal{E}_{Ey}\} = \{\mathcal{E}_{xz}, \mathcal{E}_{yz}\}. \end{aligned} \quad (6)$$

In the quasi-2D limit, we ignore the inter-layer spin-lattice coupling, so  $\mathcal{E}_{zz}$  in the  $A_1$  irrep does not enter the Hall viscosity.

Consider next the determination of  $G(\mathbf{n}, \mathbf{h})$  and  $G^{\text{eff}}(\mathbf{n}, \mathbf{h})$  for this system. For concreteness, we choose the field along the  $z$ -axis,  $\mathbf{h} = h\hat{\mathbf{z}}$ , and place  $\mathbf{n}$  in the  $xy$  plane (which is energetically preferred for this field orientation). For our purpose, we distinguish two cases: the “high symmetry” AFMs for which  $\mathbf{n}$  is aligned with a high-symmetry direction, i.e. to the  $x$  or  $y$  axes or at 45 degrees between them, and the “low symmetry” AFMs where  $\mathbf{n}$  takes any other in-plane orientation. The paramagnetic and magnetic groups for zero and nonzero fields with the above provisos are given in Table I.

For this field orientation, we are interested in  $\kappa_{xy}$  and the acoustic Faraday effect for sound waves propagating along  $\hat{\mathbf{z}}$ . Both of these are odd under time-reversal and under vertical mirrors, and hence even under their combination. This is compatible with all three cases of  $G^{\text{eff}}(\mathbf{n}, \mathbf{h})$  in a non-zero applied field (see the final column of Table I), and hence both effects should be non-zero in these situations. To determine them, we will need the PHV terms with the same symmetries, i.e. those which are odd under break time-reversal  $\mathcal{T}$  and vertical mirrors, and which are invariant under  $G^{\text{eff}}(\mathbf{n}, \mathbf{h})$ : the only compatible PHV coefficients are  $\eta_{B_1, B_2}^H$  and  $\eta_{E_x, E_y}^H$ . Other field configurations can be analyzed similarly – see SM.

*Contributing magnetic operators.*—We are now in a position to ask about the allowed forms of the  $\mathcal{O}$  operators which appear in  $\mathcal{L}_{sl}$  and which contribute to a nonzero

$\eta^H$ , as well as their correlations. The magnetic operators  $\mathcal{O}$  are polynomials of the Gaussian fields  $\mathbf{n}_\perp, \mathbf{m}_\perp$ , so that we may calculate correlators of the  $\mathcal{O}$ ’s using Wick’s theorem. We keep only those which effectively yield “mixed” correlators of  $\mathbf{m}$  and  $\mathbf{n}$ .

In the absence of a magnetic field, the PHV vanishes. Indeed, because  $\mathbf{m}$  is odd under the  $\mathcal{TX}$  and  $\mathcal{TY}$  symmetries of the AFM state, all allowed polynomials are even in  $\mathbf{m}$ . In an external magnetic field however, the uniform magnetization  $\mathbf{m}$  acquires a static component  $\mathbf{m}_0 = \chi h\hat{\mathbf{z}}$  so that  $m_x = -\chi h n_z$  to linear order in  $h$ . One can thereby obtain an odd-in-frequency contribution to the two-point  $\mathcal{O}$  correlators: this occurs in the cases for which one magnetic operator  $\mathcal{O}$  is even and the other is odd in  $\mathbf{m}_\perp$ . To lowest order, the important terms are  $\mathcal{O}_{B_1} \sim h m_z$ ,  $\mathcal{O}_{B_2} \sim n_y$ ,  $\mathcal{O}_{E_x} \sim n_z$ ,  $\mathcal{O}_{E_y} \sim h m_y$  (see SM Sec.B3) —contributions from higher powers of magnon operators are parametrically small by a factor of  $k_B T/J$  or  $v_m \delta_\alpha/J$  (see SM Sec. D). Appropriately combined, the latter give

$$\eta_{B_1, B_2}^H \sim -h \langle m_z n_y \rangle, \quad \eta_{E_x, E_y}^H \sim h \langle n_z m_y \rangle. \quad (7)$$

A careful analysis that restores the units (see SM Sec. A1) gives

$$\eta_{\Gamma\Gamma'}^H(\mathbf{q}) = \frac{\lambda_\Gamma \lambda_{\Gamma'} S^3 \chi h}{d_z a_0^2} \mathcal{D}_{\alpha(\Gamma\Gamma')}(\mathbf{q}_\perp, \omega = 0) = \frac{\gamma_{\Gamma\Gamma'}}{q_x^2 + q_y^2 + \delta_\alpha^2}, \quad (8)$$

where  $\gamma_{\Gamma\Gamma'} = \frac{h S^2 \lambda_\Gamma \lambda_{\Gamma'}}{v_m^2 g d_z a_0}$ ,  $\alpha(B_1, B_2) = y$ ,  $\alpha(E_x, E_y) = z$ , and  $\mathbf{q}_\perp$  projects the momentum  $\mathbf{q}$  to the  $xy$  plane. The factor of  $d_z$ , the inter-layer spacing in the  $z = c$  direction, is necessary to convert to bulk three-dimensional elasticity.

*Acoustic Faraday effect.*— This effect can be understood as arising from splitting of the degeneracy between right- and left-circularly polarized sound waves. This allows a transverse linearly-polarized wave propagating along  $\hat{\mathbf{z}}$  at a frequency  $\omega_{\text{ph}}$  to undergo a Faraday rotation. The Faraday rotation angle  $\Phi$  per unit length  $L$  is simply given by the difference in wavenumber between right-

and left-circularly polarized waves at a given frequency  $\omega_{\text{ph}}$ . By calculating the dispersion relation including the PHV, we find  $\Phi/L$  is related to the Hall viscosity coefficient  $\eta_{E_x E_y}^H$  through (see the SM)

$$\frac{\Phi}{L} = \frac{\eta_{E_x E_y}^H \omega_{\text{ph}}^2}{v_T^3 \rho} = \frac{\gamma_{E_x E_y} \omega_{\text{ph}}^2}{v_T^3 \rho \delta_z^2} + O(\omega_{\text{ph}}^3). \quad (9)$$

where  $\rho$  is the mass density of the lattice,  $v_T$  is the asymptotic long wavelength transverse sound wave velocity for this propagation direction, and recall  $\delta_z$  is the out-of-plane magnon gap in units of inverse length.

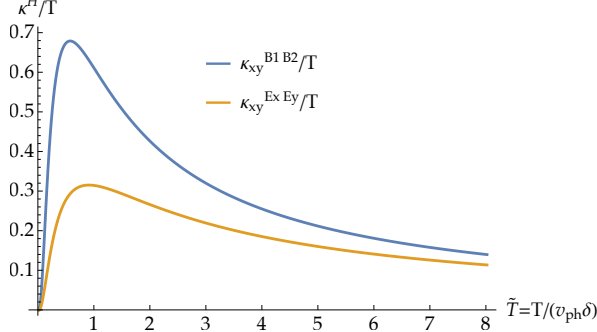


FIG. 1. Intrinsic phonon thermal Hall conductivity,  $\kappa_{xy}/T$  v.s.  $T$  (rescaled in units of  $v_{\text{ph}}\delta_\alpha$ ). Only the value of  $F_\alpha(\tilde{T})$  in Eq. (12) is plotted, and the overall coefficient not shown in the plot is set by the RHS of Eq. (13).

*Thermal Hall conductivity.*—Following Ref. [10], the intrinsic (by which we mean independent of impurities) non-collisional thermal Hall conductivity  $\kappa_{jk}$  is determined by the Berry curvature  $\Omega_{\mathbf{q},\sigma}^i$  and the phonon dispersions  $\omega_{\mathbf{q},\sigma}$ :

$$\kappa_{jk} = -\frac{1}{T} \int_0^\infty dE E^2 \sigma_{jk}(E) \frac{dn_B^{\text{eq}}(E)}{dE}, \quad (10)$$

where we defined the “conductivity”  $\sigma_{jk}$ :

$$\sigma_{jk}(E) = -\sum_\sigma \int \frac{d^3 q}{(2\pi)^3} \epsilon_{ijk} \Omega_{\mathbf{q},\sigma}^i \Theta(E - \omega_{\mathbf{q},\sigma}), \quad (11)$$

where  $\epsilon$  is the Levi-Civita tensor, the subscript  $\sigma$  labels the phonon branch, and  $n_B^{\text{eq}}$  is the Bose-Einstein distribution.

A non-zero Berry curvature  $\Omega$  is obtained by finding the phonon eigenfunctions including the PHV, which induces a vector potential in the phonon Hamiltonian (see Sec. C2 of the SM). The leading nonzero terms are linear in  $\eta^H$ , and to this order contributions to  $\kappa_H$  from  $\eta_{\Gamma\Gamma'}^H$  add—each is labeled  $\kappa_H^{\Gamma\Gamma'}$  below. Defining a dimensionless temperature  $\tilde{T} = T/(v_{\text{ph}}\delta_\alpha)$ , where  $v_{\text{ph}}$  is the mean sound velocity, we find

$$\frac{\kappa_{xy}^{\Gamma\Gamma'}}{T} \sim \frac{\gamma_{\Gamma\Gamma'}}{\rho v_{\text{ph}}} F_{\alpha(\Gamma\Gamma')}(\tilde{T}), \quad (12)$$

where  $F_{\alpha(\Gamma\Gamma')}$  is a scaling function. The detailed forms of  $F_{\alpha(\Gamma\Gamma')}(\tilde{T})$  for different  $\Gamma\Gamma'$  are given in the SM, and are numerically evaluated and plotted in Fig. 1. Importantly, we find that the temperature scaling of  $\kappa_H/T$  is sensitive to the  $\mathbf{q}$  dependence of  $\eta^H$ . If  $\eta^H$  is a constant, straightforward power counting shows that  $\kappa_H/T \sim T^{d-1}$ , where  $d$  is the spatial dimension. For  $\eta^H$  with the  $\mathbf{q}$  dependence of Eq. (8), the spin gap  $\sim \delta_\alpha$  introduces an additional scale that controls the temperature dependence, and  $\kappa_H/T$  is non-monotonic.  $\kappa_H/T$  increases from  $T = 0$  as  $T^2$ , reaches a maximum at  $T_{\text{max}} \sim v_{\text{ph}}\delta_\alpha$ . At  $T/v_{\text{ph}}\delta_\alpha \gg 1$ ,  $\kappa_H/T$  decreases as  $1/T^\zeta$ , where  $\zeta \sim 1$  (see Fig. 1).

*Summary and discussion.*—In this work, we presented a symmetry analysis of the phonon Hall viscosity and resulting phonon Berry curvature in a magnetoelastically coupled system. The procedure includes accounting for separate scales for anisotropy-induced magnon gaps and the applied magnetic field, and follows from a magnetic space group symmetry analysis. The symmetry predictions were checked for a low-energy magnon model by an explicit calculation in terms of spin correlation functions. We found that the phonon Hall viscosity  $\eta^H$  retains non-trivial dependence on the scaling variable  $\mathbf{q}\delta$ , even when the phonon momentum is small  $\mathbf{q}a_0 \ll 1$ , due to the small spin gap  $\sim \delta$ .

As an example, we modeled the cuprate Mott insulator  $\text{Sr}_2\text{CuO}_2\text{Cl}_2$  with tetragonal symmetry. We showed that PHV induces thermal Hall conductivity via both Hall viscosities  $\eta_{B_1 B_2}^H$  and  $\eta_{E_x E_y}^H$ , while the acoustic Faraday effect arises only from  $\eta_{E_x E_y}^H$ .

The treatment above implicitly uses spin-orbit coupling (SOC) throughout, in the symmetry analysis and through the forms of the spin-lattice couplings. Without SOC, one instead requires that the microscopic Hamiltonian (before any spontaneous symmetry breaking) in the absence of an applied magnetic field has a global  $\text{SO}(3)$  spin-rotation symmetry  $\text{SO}(3)_s$ . The latter acts only on spin indices, and is distinct from and independent of the space group and time-reversal symmetries, which act on coordinates, spatial derivatives, and strain indices. Under the assumption that the applied magnetic field couples only via the Zeeman interaction, then the symmetry constraints on the PHV are significantly more stringent in the absence of SOC. We forgo a general discussion here, but give a simple argument that whenever the applied magnetic field and all local ordered spin moments lie in a single plane, the PHV vanishes. Indeed, under those assumptions, all Zeeman and exchange fields are invariant under the operation  $\mathcal{T}[C_{2\hat{\mathbf{w}}}]_s$ , where the second operation is a  $C_2$  rotation *in spin space* about an axis  $\hat{\mathbf{w}}$  normal to the plane containing the spins and field. Because spin rotations do not act on the strain, this operation is indistinguishable from time-reversal symmetry in the lattice effective action, and thus PHV is prohibited.

In a real material with weak but nonzero SOC, there will be an additional smallness of the PHV due to weak SOC.

We now turn to an estimate of the magnitude of the phonon Hall effect induced by the mechanism in this paper. The characteristic energy  $v_{\text{ph}}\delta_\alpha$  and the maximum of  $\kappa_{xy}/T$  can be related to parameters that may be obtained from experiments/ab-initio calculations. The thermal conductivity is most conveniently expressed as  $\kappa_{xy}/T$  per layer and in terms of the ratio of the phonon to the magnon velocity  $\Upsilon = v_{\text{ph}}/v_m$ . In units of thermal conductance, we have:

$$\frac{d_z \kappa_{xy}^{\Gamma\Gamma'}}{T} \sim \frac{\gamma_{\Gamma\Gamma'} d_z k_B^2}{\rho v_{\text{ph}} \hbar} = \Upsilon \frac{\lambda_\Gamma \lambda_{\Gamma'}}{J v_m / d_z} \frac{h}{\rho a_0^2 d_z v_{\text{ph}}^2} \frac{k_B^2}{\hbar} \times O(1). \quad (13)$$

Here  $d_z$  is the inter-layer distance, and the numerical coefficient ( $O(1)$ ) depends on the specific microscopic model. Because the magnetoelastic couplings may be considered spatial derivatives of the (anisotropic) exchange, and the magnon velocity is also set by exchange, we expect that  $\frac{\lambda_\Gamma \lambda_{\Gamma'}}{J v_m / d_z} \lesssim 1$  (smallness due to weak SOC also enters here). It could be more precisely evaluated through ab initio calculations. The remaining factors behave as  $\frac{h}{\rho a_0^2 d_z v_{\text{ph}}^2} \sim h(C_{3\text{D}} a_0^2 d_z)^{-1}$ , where  $C_{3\text{D}}$  is the three-dimensional bulk modulus. The latter is generally an eV energy so that for a magnetic field  $B = 15$  T, i.e.  $h = g_s \mu_B B \sim 30$  K,  $h(C_{3\text{D}} a_0^2 d_z)^{-1} \sim 10^{-4}$ . For cuprates,  $\Upsilon < 1$  due to the large exchange energy. Thus, the thermal Hall conductivity due to the PHV mechanism is smaller by a factor of at least  $10^{-4}$  than measured values for cuprates.

This leaves open other mechanisms for the phonon Hall effect in the cuprates. It is possible that the effects of the PHV are enhanced by impurity scattering of phonons, not included here (see a recent preprint [22] for discussion on related issues). There might also be alternative mechanisms to generate larger PHV, e.g. from charged impurities. Finally, phonons may acquire chirality via skew scattering of phonons from spins. This mechanism, which is independent of the PHV, requires a true non-equilibrium transport treatment.

A partial means to distinguish between these possibilities is to compare directly the acoustic Faraday and phonon Hall effect measurements to see if they can be consistently related to comparable PHVs. Beyond the cuprates, the above discussion can be easily extended to any antiferromagnet, and may be used to guide a search for large PHVs. At a general level, it is clear that large spin-orbit coupling or non-coplanar magnetic order (which evades the weak SOC smallness), and large magnetoelastic couplings are beneficial for enhancing the PHV. We expect our results will be useful to guide future experiments and computations in this active area.

We acknowledge Léo Mangeolle for a collaboration on a related project and helpful discussions. M.Y. also bene-

fited from collaborations with Natalia Perkins and Rafael Fernandes on a past work on phonon Hall viscosity. L.B. was supported by the DOE, Office of Science, Basic Energy Sciences under Award No. DE-FG02-08ER46524. M.Y. is supported in part by the Gordon and Betty Moore Foundation through Grant GBMF8690 to UCSB and by the National Science Foundation under Grant No. NSF PHY-1748958. L.S. acknowledges funding from the European Research Council (ERC) under the European Union's Horizon 2020 research and innovation program (Grant agreement No. 853116, "TRANSPORT") as well as from the ToRe IDEX-Lyon breakthrough program.

- 
- [1] Maissam Barkeshli, Suk Bum Chung, and Xiao-Liang Qi, "Dissipationless phonon hall viscosity," *Phys. Rev. B* **85**, 245107 (2012).
  - [2] Thomas I. Tügel and Taylor L. Hughes, "Hall viscosity and the acoustic faraday effect," *Phys. Rev. B* **96**, 174524 (2017).
  - [3] Hassan Shapourian, Taylor L. Hughes, and Shinsei Ryu, "Viscoelastic response of topological tight-binding models in two and three dimensions," *Phys. Rev. B* **92**, 165131 (2015).
  - [4] J. E. Avron, R. Seiler, and P. G. Zograf, "Viscosity of quantum hall fluids," *Phys. Rev. Lett.* **75**, 697–700 (1995).
  - [5] J. E. Avron, "Odd viscosity," *Journal of Statistical Physics* **92**, 543–557 (1998).
  - [6] N. Read, "Non-abelian adiabatic statistics and hall viscosity in quantum hall states and  $p_x + ip_y$  paired superfluids," *Phys. Rev. B* **79**, 045308 (2009).
  - [7] N. Read and E. H. Rezayi, "Hall viscosity, orbital spin, and geometry: Paired superfluids and quantum hall systems," *Phys. Rev. B* **84**, 085316 (2011).
  - [8] Barry Bradlyn, Moshe Goldstein, and N. Read, "Kubo formulas for viscosity: Hall viscosity, ward identities, and the relation with conductivity," *Phys. Rev. B* **86**, 245309 (2012).
  - [9] A. Sytcheva, U. Löw, S. Yasin, J. Wosnitza, S. Zherlitsyn, P. Thalmeier, T. Goto, P. Wyder, and B. Lüthi, "Acoustic faraday effect in  $\text{tb}_3\text{ga}_5\text{o}_{12}$ ," *Phys. Rev. B* **81**, 214415 (2010).
  - [10] Tao Qin, Jianhui Zhou, and Junren Shi, "Berry curvature and the phonon hall effect," *Phys. Rev. B* **86**, 104305 (2012).
  - [11] Yuval Vinkler-Aviv and Achim Rosch, "Approximately quantized thermal hall effect of chiral liquids coupled to phonons," *Phys. Rev. X* **8**, 031032 (2018).
  - [12] Xiaou Zhang, Yinhan Zhang, Satoshi Okamoto, and Di Xiao, "Thermal hall effect induced by magnon-phonon interactions," *Phys. Rev. Lett.* **123**, 167202 (2019).
  - [13] Jing-Yuan Chen, Steven A. Kivelson, and Xiao-Qi Sun, "Enhanced thermal hall effect in nearly ferroelectric insulators," *Phys. Rev. Lett.* **124**, 167601 (2020).
  - [14] Mengxing Ye, Rafael M. Fernandes, and Natalia B. Perkins, "Phonon dynamics in the kitaev spin liquid," *Phys. Rev. Research* **2**, 033180 (2020).
  - [15] Takuma Saito, Kou Misaki, Hiroaki Ishizuka, and Naoto Nagaosa, "Berry phase of phonons and thermal hall effect

- in nonmagnetic insulators,” *Phys. Rev. Lett.* **123**, 255901 (2019).
- [16] M. Boiteux, P. Doussineau, B. Ferry, J. Joffrin, and A. Levelut, “Acoustical faraday effect in antiferromagnetic  $\text{Cr}_2\text{O}_3$ ,” *Phys. Rev. B* **4**, 3077–3088 (1971).
  - [17] Gaël Grissonnanche, Anaëlle Legros, Sven Badoux, Étienne Lefrançois, Victor Zatzko, Maude Lizaire, Francis Laliberté, Adrien Gourgout, Jianshi Zhou, Sunseng Pyon, Tomohiro Takayama, Hidenori Takagi, Shimpei Ono, Nicolas Doiron-Leyraud, and Louis Taillefer, “Giant thermal hall conductivity in the pseudogap phase of cuprate superconductors,” *Nature* **571**, 376–380 (2019).
  - [18] Marie-Eve Boulanger, Gaël Grissonnanche, Sven Badoux, Andréanne Allaire, Étienne Lefrançois, Anaëlle Legros, Adrien Gourgout, Maxime Dion, C. H. Wang, X. H. Chen, R. Liang, W. N. Hardy, D. A. Bonn, and Louis Taillefer, “Thermal hall conductivity in the cuprate mott insulators  $\text{Nd}_2\text{CuO}_4$  and  $\text{Sr}_2\text{CuO}_2\text{Cl}_2$ ,” *Nature Communications* **11**, 5325 (2020).
  - [19] G. Grissonnanche, S. Thériault, A. Gourgout, M. E. Boulanger, E. Lefrançois, A. Ataei, F. Laliberté, M. Dion, J. S. Zhou, S. Pyon, T. Takayama, H. Takagi, N. Doiron-Leyraud, and L. Taillefer, “Chiral phonons in the pseudogap phase of cuprates,” *Nature Physics* (2020), 10.1038/s41567-020-0965-y.
  - [20] Symmetry allows additional PHV terms which are not expressed solely in terms of the strain but also in terms of the time derivative of the rotation  $\mathcal{M}_{ij} = \frac{1}{2}(\partial_i u_j - \partial_j u_i)$ . Such terms, however, cannot be induced by conventional magnetoelastic coupling which involves strain only.
  - [21] Mois I. Aroyo, Asen Kirov, Cesar Capillas, J. M. Perez-Mato, and Hans Wondratschek, “Bilbao crystallographic server. ii. representations of crystallographic point groups and space groups,” *Acta Crystallographica Section A Foundations of Crystallography* **62**, 115–128 (2006).
  - [22] Haoyu Guo and Subir Sachdev, “Extrinsic phonon thermal Hall transport from Hall viscosity,” *arXiv e-prints*, arXiv:2103.02614 (2021), arXiv:2103.02614 [cond-mat.str-el].
  - [23] Subir Sachdev, “Quantum phase transitions,” (2009), 10.1017/cbo9780511973765.
  - [24] George F. Koster, *Properties of the thirty-two point groups* (M.I.T. Press, Cambridge, Mass., 1963) p. 104 p.
  - [25] T. Yildirim, A. B. Harris, Amnon Aharony, and O. Entin-Wohlman, “Anisotropic spin hamiltonians due to spin-orbit and coulomb exchange interactions,” *Phys. Rev. B* **52**, 10239–10267 (1995).
  - [26] L. Benfatto, M. B. Silva Neto, A. Gozar, B. S. Dennis, G. Blumberg, L. L. Miller, Seiki Komiyama, and Yoichi Ando, “Field dependence of the magnetic spectrum in anisotropic and dzyaloshinskii-moriya antiferromagnets. ii. raman spectroscopy,” *Phys. Rev. B* **74**, 024416 (2006).

## SUPPLEMENTAL MATERIAL

In the supplemental material (SM), we present additional details of the modeling and computations.

Sec. A reviews the detailed derivation of the correlation function of staggered and ferromagnetic field in Eq. (4) of the main text based on the non-linear sigma model formulation. Summaries of the point group symmetry operations and symmetry allowed magnetic operators in the spin-lattice coupling [Eq. (2) in main the text] are given in Sec. B. In Sec. C, we show details to analyze the acoustic Faraday and phonon thermal Hall effects.

For completeness, a few additional considerations are presented. We first show that the next order in  $1/S$  contribution to  $\eta^H$  from two magnon fluctuations are small in magnitude at low temperature, and can thus be ignored (Sec. D). Next, we show the microscopic Hamiltonian allowed by crystal symmetry in Sec. E. A comparison between the microscopic Hamiltonian and the low energy effective action analysis is helpful to infer the spin gap and reveal the microscopic origin of the relevant spin-lattice coupling for a material. Finally, the phonon Hall viscosity with in-plane magnetic field is discussed (Sec. F).

### A: Non-linear sigma model formulation of spin dynamics

In this section, we derive the low energy field theory and correlations function for the antiferromagnetic state. Before doing so, we address briefly the validity of the low energy approach. Since  $\eta_{\Gamma\Gamma'}^H(\mathbf{q})$  arises from virtual rather than on-shell magnetic excitations, there is no kinetic constraint, and spin fluctuations at all energies may contribute to it. However, high energy magnetic excitations are still polynomially suppressed by their energies, and indeed we have checked that, within a full spin wave calculation, contributions from high-energy magnons are suppressed by additional powers of  $k_B T/J$  with respect to the low energy ones. This justifies the low energy approach.

We proceed with the standard non-linear sigma model (NLSM) formulation for collinear antiferromagnets and obtain the two-point correlation functions for a staggered field ( $\mathbf{n}$ ) and a ferromagnetic field ( $\mathbf{m}$ ) in an external magnetic field ( $\mathbf{h}$ ) in a two-dimensional (2d) spin system. It gives Eq. (4) in the main text.

Following Ref. [23], the coherent state path integral for a Heisenberg spin with spin value  $S$  at site  $\mathbf{r}$  can be obtained in the basis of the (unit) vector field  $\mathbf{e}_{\mathbf{r}}$ , which is defined through  $\hat{\mathbf{S}}_{\mathbf{r}}|\mathbf{e}_{\mathbf{r}}\rangle = S\mathbf{e}_{\mathbf{r}}|\mathbf{e}_{\mathbf{r}}\rangle$  and  $|\mathbf{e}_{\mathbf{r}}|^2 = 1$ . For a collinear antiferromagnet, the ground state has spins oriented in opposite directions on the two sublattices (defined as  $A$ ,  $B$  sublattice hereafter). The low energy spin dynamics can be described by a set of continuous fields, which include the staggered  $\mathbf{n} \sim \mathbf{e}_A - \mathbf{e}_B$  and uniform  $\mathbf{m} \sim \mathbf{e}_A + \mathbf{e}_B$  magnetization fields, where the subscript  $A$ ,  $B$  label the  $A$ ,  $B$  sublattice. To be accurate, we use

$$\mathbf{e}_{\mathbf{r}} = (-1)^{\mathbf{r}} \mathbf{n}_{\mathbf{r}} \sqrt{1 - (\mathbf{m}_{\mathbf{r}})^2} + \mathbf{m}_{\mathbf{r}}, \quad (\text{A1})$$

where  $\mathbf{m}$  is the uniform magnetization per site in units of the saturation magnetization ( $= S$  semiclassically), and  $(-1)^{\mathbf{r}}$  is a sign equal to  $+1$  on the  $A$  sublattice and  $-1$  on the  $B$  sublattice. The effective spin action (for the isotropic Heisenberg model) is

$$\begin{aligned} \mathcal{Z}_s &= \int \mathcal{D}\mathbf{n} \mathcal{D}\mathbf{m} \delta(\mathbf{n}^2 - 1) \delta(\mathbf{n} \cdot \mathbf{m}) \exp(-\mathcal{S}_s) \\ \mathcal{S}_s &= \frac{1}{2} \int dx dy d\tau \left\{ \frac{v_m}{ga_0} [(\nabla_x \mathbf{n})^2 + (\nabla_y \mathbf{n})^2] + \frac{v_m g S^2}{a_0^3} \mathbf{m}^2 - \frac{2iS}{a_0^2} \mathbf{m} \cdot \left( \mathbf{n} \times \frac{\partial \mathbf{n}}{\partial \tau} - i\mathbf{h} \right) \right\}, \end{aligned} \quad (\text{A2})$$

In the second equation, we introduced the spin wave (magnon) velocity  $v_m \sim Ja_0 S$ , with  $a_0$  the lattice constant, and the coefficient of  $\mathbf{m}^2$  defines the coupling  $g$  with  $g \sim S^{-1}$ . We ignore the spin wave velocity along  $\hat{\mathbf{z}}$  because of the much weaker interlayer spin exchange. In the standard procedure the Gaussian field  $\mathbf{m}$  is then integrated out. As  $\mathbf{m}$  does not have its own dynamics, the action can be obtained by replacing  $\mathbf{m}$  with its saddle-point solution,

$$\mathbf{m} = \chi \left( i\mathbf{n} \times \frac{\partial \mathbf{n}}{\partial \tau} + \mathbf{h} - \mathbf{n}(\mathbf{n} \cdot \mathbf{h}) \right), \quad (\text{A3})$$

which defines the susceptibility  $\chi = a_0/v_m g S$ .

Below, we consider an antiferromagnet with the Néel vector along the  $x$ -axis, i.e.  $\lim_{h \rightarrow 0} \langle \mathbf{n} \rangle = n_0 \hat{\mathbf{x}}$ , and the magnetic field perpendicular to the Néel vector. As the spin-lattice coupling is most transparently expressed in terms of  $\mathbf{n}$ ,  $\mathbf{m}$  fields to reveal the symmetries, our goal below is to obtain the correlators of  $\mathbf{n}$  and  $\mathbf{m}$ . The staggered field can be parameterized by  $\mathbf{n} = \{n_0, n_y, n_z\} = (n_0, \mathbf{n}_{\perp})$ , where  $n_0 = \sqrt{1 - \mathbf{n}_{\perp}^2}$  is the order parameter, and  $n_{y,z}$  are

transverse fluctuations (spin waves). Note from Eq. (A3) that  $\mathbf{m}$  can be decomposed into components of zeroth order in  $\mathbf{h}$  and first order in  $\mathbf{h}$ . The first-order term includes the static part, i.e. the field induced uniform magnetization  $\chi\mathbf{h}$  as well as  $-\chi\mathbf{n}(\mathbf{n}\cdot\mathbf{h})$  to satisfy the constraint  $\mathbf{n}\cdot\mathbf{m}=0$  at first order in  $\mathbf{h}$ . We then define  $\mathbf{m}$  through  $\mathbf{m}=\chi\mathbf{h}+\mathbf{m}_\perp$ , and within linear spin wave theory,  $m_x=-\chi n_x(\mathbf{n}\cdot\mathbf{h})\rightarrow-\chi n_0(n_y h_y+n_z h_z)$ . Plugging  $\chi\mathbf{h}$  and  $m_x$  to  $\mathcal{S}_s$  into Eq. (A2), we obtain the Lagrangian density in terms of  $\mathbf{n}_\perp$  and  $\mathbf{m}_\perp$ .

With an external field  $\mathbf{h}=h\hat{\mathbf{z}}$ .

$$\mathcal{S}_s = \frac{1}{2} \sum_{\mathbf{k},n} \begin{pmatrix} n_y & m_y & n_z & m_z \end{pmatrix}_{\mathbf{k},n} \begin{pmatrix} \frac{1}{gv_m a_0} (v_m^2 \mathbf{k}^2 + \Delta_y^2) & \frac{v_m g S^2}{a_0^2} & -\frac{S\omega_n}{a_0^2} & -\frac{S\omega_n}{a_0^2} \\ \frac{S\omega_n}{a_0^2} & \frac{1}{gv_m a_0} (v_m^2 \mathbf{k}^2 + h^2 + \Delta_z^2) & \frac{v_m g S^2}{a_0^2} & \frac{v_m g S^2}{a_0^2} \end{pmatrix} \begin{pmatrix} n_y \\ m_y \\ n_z \\ m_z \end{pmatrix}_{-\mathbf{k},-n} \quad (\text{A4})$$

Here, the Fourier transform follows the convention  $f_{\mathbf{k}} = \frac{1}{L} \int d\mathbf{x} dy e^{-i\mathbf{k}\cdot\mathbf{x}} f(\mathbf{x})$ , where  $L$  is the linear size of the sample ( $\int d\mathbf{x} dy 1 = L^2$ ). Inverting the matrix, we obtain the correlator:

$$\langle T_\tau \begin{pmatrix} n_\alpha \\ m_{\bar{\alpha}} \end{pmatrix}_{\mathbf{k}} \begin{pmatrix} n_\alpha & m_{\bar{\alpha}} \end{pmatrix}_{-\mathbf{k}} \rangle_{\omega_n} = \mathcal{D}_\alpha(\mathbf{k}, \omega_n) \begin{pmatrix} v_m g a_0 & \frac{\omega_n a_0^2}{S} \epsilon_{x\alpha\bar{\alpha}} \\ -\frac{\omega_n a_0^2}{S} \epsilon_{x\alpha\bar{\alpha}} & \frac{\omega_{\alpha,\mathbf{k}}^2 a_0^3}{v_m g S^2} \end{pmatrix}. \quad (\text{A5})$$

Here  $a_0$  is the lattice constant,  $\mathcal{D}_\alpha^{-1}(\mathbf{k}, \omega_n) = \omega_n^2 + \omega_{\alpha,\mathbf{k}}^2$ ,  $\omega_{\alpha,\mathbf{k}}$  is the dispersion for the magnon branch  $\alpha \in \{y, z\}$ , such that  $\omega_{\alpha,\mathbf{k}} = v_m \sqrt{k_x^2 + k_y^2 + \delta_\alpha^2}$ , the spin gap is determined by the XYZ anisotropy ( $\sim \Delta_\alpha$ ) and external field strength  $h$  by  $\delta_y = \Delta_y/v_m$ ,  $\delta_z = \sqrt{\Delta_z^2 + h^2}/v_m$ .

With an external field  $\mathbf{h}=h\hat{\mathbf{y}}$ . Because here also  $\mathbf{h} \perp \langle \mathbf{n} \rangle$ , the situation is similar to that when  $\mathbf{h}=h\hat{\mathbf{z}}$ . The effective spin action simply changes according to  $\Delta_y^2 \rightarrow (\Delta_y^2 + h^2)$ ,  $\Delta_z^2 + h^2 \rightarrow \Delta_z^2$  in Eq. (A4). Consequently,  $\delta_y = \sqrt{\Delta_y^2 + h^2}/v_m$  and  $\delta_z = \Delta_z/v_m$ .

### 1. Normalization of operators, Fourier conventions, etc.

Here we discuss the conventions used to obtain the Hall viscosity form given in the main text, Eq. (8). We begin with a consideration of units. Hall viscosity, Eq. (1), is defined as a coefficient in a three-dimensional elastic theory. We employ Fourier conventions for the strain which are appropriate to a three-dimensional system, so that

$$\mathcal{E}_{\Gamma,\mathbf{q}} = \frac{1}{\sqrt{V}} \int d^3\mathbf{x} \mathcal{E}_\Gamma(\mathbf{x}) e^{-i\mathbf{q}\cdot\mathbf{x}}, \quad \mathcal{E}_\Gamma(\mathbf{x}) = \frac{1}{\sqrt{V}} \sum_{\mathbf{q}} e^{i\mathbf{q}\cdot\mathbf{x}} \mathcal{E}_{\Gamma,\mathbf{q}}, \quad (\text{A6})$$

where  $V$  is the volume of the system. With this convention, since the real space strain  $\mathcal{E}_\Gamma(\mathbf{x})$  is dimensionless,  $\mathcal{E}_{\Gamma,\mathbf{q}}$  has dimensions of  $1/\sqrt{V}$ . Then Eq. (1) implies that, because the action is dimensionless,  $\eta^H$  has units of inverse volume.

Next consider the spin-lattice coupling in Eq. (2). The Lagrange density has units of energy density, so that the combination  $\lambda_\Gamma \mathcal{O}_\Gamma$  must have units of energy density. We assigned energy units to  $\lambda$ , which requires  $\mathcal{O}_\Gamma$  to scale as a number density. How this is precisely realized depends upon our treatment of the third dimension. We will proceed here with the treatment as a discrete layered system, so that the corresponding action is  $\mathcal{S}_{sl} = \sum_z \int d\mathbf{x} dy \mathcal{L}_{sl}$ . Then  $\mathcal{O}_\Gamma$  has units of inverse length squared. Let us see how these factors appear in the derivation of Eq. (8).

All the contributions to the spin-lattice coupling arise microscopically from expressions (see Sec. E) of the form  $\sum_{\mathbf{r}} \lambda_\Gamma \mathcal{E}_\Gamma(SS)_{\Gamma,\mathbf{r}}$ , where  $(SS)_{\Gamma,\mathbf{r}}$  represents a sum of spin bilinears in the vicinity of site  $\mathbf{r}$ . We convert this to continuum fields using Eq. (A1) and  $\sum_{\mathbf{r}} \rightarrow a_0^{-2} \sum_z \int d\mathbf{x} dy$ , which gives

$$\mathcal{O}_{B_1} = \frac{S^2 \chi h m_z}{a_0^2}, \quad \mathcal{O}_{B_2} = \frac{S^2 n_0 n_y}{a_0^2}, \quad \mathcal{O}_{E_x} = \frac{S^2 n_0 n_z}{a_0^2}, \quad \mathcal{O}_{E_y} = \frac{S^2 \chi h m_y}{a_0^2}. \quad (\text{A7})$$

The factors of  $S^2, \chi, 1/a_0^2, n_0$  are subsumed in the  $\sim$  in the discussion of the main text. Now consider evaluating Eq. (3). We must take care due to the combination of the three-dimensional Fourier transform convention for elasticity with our two-dimensional magnetism theory. Consider the  $B_1 - B_2$  contribution. What actually arises in the effective action is

$$\mathcal{S}_{sl}^{B_1 B_2} = \sum_{z,z'} \int d\mathbf{x} dy d\tau \int d\mathbf{x}' dy' d\tau' \lambda_{B_1} \lambda_{B_2} \mathcal{E}_{B_1}(x, y, z, \tau) \mathcal{E}_{B_2}(x', y', z', \tau') \langle \mathcal{O}_{B_1}(x, y, z, \tau) \mathcal{O}_{B_2}(x', y', z', \tau') \rangle. \quad (\text{A8})$$



Since we assume no spin correlations between layers, the summand is non-zero only for  $z' = z$ . Inserting the three-dimensional Fourier expression of Eq. (A6) for the strains gives

$$\mathcal{S}_{sl}^{B_1 B_2} = \frac{1}{V} \sum_z \sum_{\mathbf{q}, \mathbf{q}'} \int dx dy d\tau \int dx' dy' d\tau' \lambda_{B_1} \lambda_{B_2} \mathcal{E}_{B_1, \mathbf{q}}(\tau) \mathcal{E}_{B_2, \mathbf{q}'}(\tau') e^{i(\mathbf{q}_\perp \cdot \mathbf{x}_\perp + \mathbf{q}'_\perp \cdot \mathbf{x}'_\perp)} e^{i(q_z + q'_z)z} \langle \mathcal{O}_{B_1}(x, y, \tau) \mathcal{O}_{B_2}(x', y', \tau') \rangle. \quad (\text{A9})$$

The sum over  $z$  gives  $N_z \delta_{q_z + q'_z, 0}$ , where  $N_z = L_z/d_z$  is the number of layers. Combining this with the  $1/V$  prefactor gives  $\frac{L_z}{d_z} \frac{1}{V} = \frac{1}{d_z L^2}$ . We can now use the  $1/L^2$  to form the prefactors of the *two-dimensional* Fourier transform for each of the two  $\mathcal{O}$  operators. Hence

$$\mathcal{S}_{sl}^{B_1 B_2} = \sum_{\mathbf{q}_\perp, \mathbf{q}'_\perp} \sum_{q_z} \frac{\lambda_{B_1} \lambda_{B_2}}{d_z} \int d\tau d\tau' \mathcal{E}_{B_1, \mathbf{q}}(\tau) \mathcal{E}_{B_2, \mathbf{q}'}(\tau') \langle \mathcal{O}_{B_1, -\mathbf{q}_\perp}(\tau) \mathcal{O}_{B_2, -\mathbf{q}'_\perp}(\tau') \rangle \quad (\text{A10})$$

Due to momentum conservation,  $\mathbf{q}'_\perp = -\mathbf{q}_\perp$  is the only non-zero correlator, and we obtain using Eq. (A7) finally

$$\eta_{B_1, B_2}^H(\mathbf{q}) = \frac{\lambda_{B_1} \lambda_{B_2}}{d_z} \frac{S^2 \chi h}{a_0^2} \frac{S^2 n_0}{a_0^2} \times [-i \partial_\omega \langle m_z, -\mathbf{q}_\perp | n_y, \mathbf{q}_\perp \rangle_{\omega_n \rightarrow -i\omega + 0^+}]. \quad (\text{A11})$$

Inserting Eq. (4) for the  $m_z - n_y$  correlation function inside the square bracket, one obtains the result in Eq. (8) for  $\Gamma = B_1$ ,  $\Gamma' = B_2$ .

We took some pains to present this in great detail for clarity, but the result can also be understood schematically on dimensional grounds: the three-dimensional Fourier transform differs from the two-dimensional one by a factor of the inverse of the square root of a length in the  $z$  direction. Converting the 2d to 3d Fourier conventions for the two  $\mathcal{O}$  operators appearing at second order in the spin-lattice coupling, one obtains an overall factor of  $1/d_z$ . This is the factor in the first term in Eq. (A11). The remaining factors were explained previously as arising from the conversion from the lattice to the 2d continuum theory.

We note furthermore that it would have been possible to formulate the magnetic correlations in three dimensions as well, which is in a sense more general, and would also avoid some of this confusion. We opted for the present formulation in order to emphasize, as discussed in the main text, that the results apply to any three-dimensional structure composed of such 2d layers, and that no three-dimensional magnetic correlations are required to induce the desired PHV terms, even those which involve the inherently three-dimensional  $E_x, E_y$  strains.

## B: Group theory analysis

Here, the relevant symmetry groups and symmetry operations on the strain and spin fields are listed for reference. We consider the example discussed in the main text, i.e. a crystal with layer group symmetry  $P4/mmm$  (number 61 of layer group). The symmetry allowed magnetic operators that appear in the spin-lattice coupling [Eq. (2) in the main text] are also presented in Tabs. III and IV.

### 1. List of point group symmetry operations

The generators of the point group symmetry for the underlying crystal,  $D_{4h}$ , are  $D_{4h} = \langle C_{4z}, \sigma_h, \sigma_v \rangle$ . They give 16 point group elements:  $D_{4h} = \{\text{Id}, 2C_{4z}, C_{2z}, 2C'_2, 2C''_2, i, \sigma_h, 2\sigma_v, 2\sigma_d, 2S_4\}$  [24]. Here Id denotes the identity.  $2C'_2$  denotes the two  $\pi$  rotation transformations, around the  $\hat{x}$  or  $\hat{y}$  axes, respectively.  $2C''_2$  denotes the two  $\pi$  rotations around the diagonal axes  $\hat{a} = \frac{1}{\sqrt{2}}(\hat{x} + \hat{y})$  and  $\hat{b} = \frac{1}{\sqrt{2}}(-\hat{x} + \hat{y})$ , respectively.  $\sigma_v$  and  $\sigma_d$  are mirror transformations with a mirror plane perpendicular to the  $xy$  plane, whose normal direction is along  $\hat{x}, \hat{y}$  and diagonal axis  $\hat{a}, \hat{b}$ , respectively.  $\sigma_h$  is a horizontal mirror reflection. The convention is shown in Fig. 2, such that the inversion transformation  $i$  can be obtained from  $i = C_{2\alpha} \sigma_\alpha$ , where  $C_{2\alpha} = C_{2x, 2y, 2z, 2a, 2b}$ ,  $\sigma_\alpha = \sigma_{vx, vy, h, da, db}$ . Here,  $\alpha = x, y, z, a, b$  denotes the axis of two-fold rotation for  $C_{2\alpha}$ , and the axis is also the normal vector of mirror plane for the respective  $\sigma_\alpha$ , with  $\alpha = vx, vy, h, da, db$ .

An external field  $\mathbf{h} = h\hat{z}$  breaks the point group  $D_{4h}$  down to  $C_{4h} = \langle C_{4z}, \sigma_h \rangle = \{E, 2C_{4z}, C_{2z}, i, \sigma_h, 2S_4\}$  through the Zeeman term  $H_Z = \mathbf{h} \cdot \sum_{\mathbf{r}} \mathbf{S}_{\mathbf{r}}$ . In terms of the antiunitary symmetries,  $\mathcal{T}$  is broken, while the Zeeman term is invariant under the antiunitary symmetries  $2\mathcal{T}C'_2 \oplus 2\mathcal{T}C''_2 \oplus 2\mathcal{T}\sigma_v \oplus 2\mathcal{T}\sigma_d$ . This gives the black-white magnetic point group  $4/m'm' = (C_{4h} + \mathcal{T} \times (D_{4h} - C_{4h}))$  as listed in Tab. I.

An external field  $\mathbf{h} = h\hat{\mathbf{y}}$  breaks  $D_{4h}$  down to  $C'_{2h} = \langle C_{2y}, i \rangle = \{E, C_{2y}, i, \sigma_{vy}\}$ , whose abstract group structure is the same as that of  $C_{2h}$ . It also preserves the antiunitary symmetries  $\mathcal{T}C_{2z} \oplus \mathcal{T}\sigma_h \oplus \mathcal{T}\sigma_{vx} \oplus \mathcal{T}C_{2x}$ , which can be generated by e.g.  $\mathcal{T}C_{2z}$  and  $C'_{2h}$ .

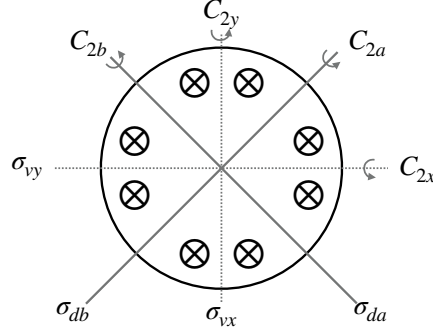


FIG. 2. Point group symmetry transformations for  $D_{4h}$ . The label  $\otimes$  denotes horizontal mirror symmetry  $\sigma_h$  that relates  $\times$  and  $\circ$ .

## 2. Symmetry operations

The point group symmetry operations acting on the strain field  $\mathcal{E}_\Gamma$ , the spin vector  $\mathbf{S}$ , the lattice coordinate  $\{x, y, z\}$ , the continuous spin fields  $\mathbf{n}, \mathbf{m}$  are listed in Table. II. For brevity, only the point group symmetry generators listed in Tab. I and Tab. V are shown.

	$C_{4z}$	$\sigma_{vx}$	$\sigma_h$	$i$	$C_{2z}$	$C_{2y}$	$C_{2x}$
$\mathcal{E}_{xx} + \mathcal{E}_{yy}$ ( $\mathcal{E}_{A_1}$ )							
$\mathcal{E}_{xx} - \mathcal{E}_{yy}$ ( $\mathcal{E}_{B_1}$ )	$-\mathcal{E}_{xx} + \mathcal{E}_{yy}$						
$\mathcal{E}_{xy}$ ( $\mathcal{E}_{B_2}$ )	$-\mathcal{E}_{xy}$	$-\mathcal{E}_{xy}$				$-\mathcal{E}_{xy}$	$-\mathcal{E}_{xy}$
$\{\mathcal{E}_{xz}, \mathcal{E}_{yz}\}$ ( $\mathcal{E}_E$ )	$\{-\mathcal{E}_{yz}, \mathcal{E}_{xz}\}$	$\{-\mathcal{E}_{xz}, \mathcal{E}_{yz}\}$	$\{-\mathcal{E}_{xz}, -\mathcal{E}_{yz}\}$		$\{-\mathcal{E}_{xz}, -\mathcal{E}_{yz}\}$	$\{\mathcal{E}_{xz}, -\mathcal{E}_{yz}\}$	$\{-\mathcal{E}_{xz}, \mathcal{E}_{yz}\}$
$\{S_x, S_y\}$	$\{-S_y, S_x\}$	$\{S_x, -S_y\}$	$\{-S_x, -S_y\}$		$\{-S_x, -S_y\}$	$\{-S_x, S_y\}$	$\{S_x, -S_y\}$
$S_z$		$-S_z$				$-S_z$	$-S_z$
$\{x, y\}$	$\{-y, x\}$	$\{-x, y\}$		$\{-x, -y\}$	$\{-x, -y\}$	$\{-x, y\}$	$\{x, -y\}$
$z$			$-z$	$-z$		$-z$	$-z$
$n_x/m_x$	$-n_y/-m_y$		$-n_x/-m_x$		$-n_x/-m_x$	$-n_x/-m_x$	
$n_y/m_y$	$n_x/m_x$	$-n_y/-m_y$	$-n_y/-m_y$		$-n_y/-m_y$		$-n_y/-m_y$
$n_z/m_z$		$-n_z/-m_z$				$-n_z/-m_z$	$-n_z/-m_z$

TABLE II. Symmetry transformation of the elastic strain tensor, spin vector, lattice coordinates, and continuous spin fields. The first row lists the important point group transformations to find the magnetic space group generators discussed above. The blank space in the table denotes the variable is invariant under the corresponding transformation. Note that from the relations  $iC_{2\alpha} = \sigma_\alpha$  and  $C_{2\alpha}C_{2\beta} = C_{2\gamma}$ ,  $C_{2\alpha}\sigma_\beta = \sigma_\gamma$ , where  $C_{2\alpha} = C_{2x, 2y, 2z, 2a, 2b}$ ,  $\sigma_\alpha = \sigma_{vx, vy, h, da, db}$  and  $\alpha, \beta, \gamma$  are mutually orthogonal basis, other symmetry transformations not listed can be generated.

## 3. Symmetry allowed spin-lattice coupling

Based on Table II, it is straightforward to classify polynomials of  $n_\mu, m_\mu$  that couples to the strain field by irreps. This is given in Table III. Note that we restricted our list to terms without spatial derivatives, as these suffer additional suppression by temperature factors well below the Debye temperature. Furthermore, we kept terms only to linear order in  $m_x$ , because in the spin wave expansion,  $m_x$ , being longitudinal, is already quadratic in the low energy transverse fields at zeroth order in  $h$ .

	$n$	$nn$	$mm$	$mmm$
$\mathcal{O}_{B_1}$	$n_y n_y, n_z n_z$	$m_y m_y, m_z m_z$	$n_y m_x m_y, n_z m_x m_z$	
$\mathcal{O}_{B_2}$	$n_y$	$m_x m_y$	$n_y m_y / z, m_y / z, n_z m_y m_z$	
$\mathcal{O}_{E_x}$	$n_z$	$m_x m_z$	$n_z m_y / z, m_y / z, n_y m_y m_z$	
$\mathcal{O}_{E_y}$	$n_y n_z$	$m_y m_z$	$n_y m_x m_z, n_z m_x m_y$	

TABLE III. Operators arranged by irrep for the high symmetry antiferromagnet such that Eq. (2) in the main text is invariant under  $G(\hat{\mathbf{x}}, \mathbf{0})$ . Other factors, e.g.  $S^2, \chi, 1/a_0^2, n_0$ , have been omitted in the table.

As described in the text, the operators can be expressed in terms of  $\mathbf{n}_\perp$  and  $\mathbf{m}_\perp$  using the NLSM constraints, after taking into account an external Zeeman field  $\mathbf{h}$ . This leads to the forms in Table IV by replacing  $m_z = \chi h + m_z$ ,  $m_x = m_x = -\chi n_z h$ .

	$n$	$nn$	$mm$	$mmm$
$\mathcal{O}_{B_1}$	$n_y n_y, n_z n_z$	$h m_z$		
$\mathcal{O}_{B_2}$	$n_y$	$-h n_z m_y$	$h n_y m_z, h n_z m_y$	
$\mathcal{O}_{E_x}$	$n_z$	$-h n_z m_z$	$h n_z m_z, h n_y m_y$	
$\mathcal{O}_{E_y}$	$n_y n_z$	$h m_y$		

TABLE IV. Magnetic operators up to quadratic order in the transverse spin wave fluctuations in the high symmetry AFM in the presence of a small field along the  $z$ -axis. Other factors, e.g.  $S^2, \chi, 1/a_0^2, n_0$ , have been omitted in the table. See Eq. (A7) for the complete expression of  $\mathcal{O}$  at linear order in  $n_\mu, m_\mu$ .

### C: Experimental Implications

Our starting point is the effective phonon Lagrangian. In Fourier space, it reads  $\mathcal{L}_{ph} = \sum_{\mathbf{q}} \mathcal{L}_{ph}^{(0)}(\mathbf{q}) + \mathcal{L}_{PHV}(\mathbf{q})$ , where

$$\mathcal{L}_{ph}(\mathbf{q}) = \frac{1}{2} \rho \dot{\mathbf{u}}_{-\mathbf{q}}^T \dot{\mathbf{u}}_{\mathbf{q}} - \frac{1}{2} \mathbf{u}_{-\mathbf{q}}^T \mathbf{M}_{\mathbf{q}} \mathbf{u}_{\mathbf{q}} + \dot{\mathbf{u}}_{-\mathbf{q}}^T \mathbf{A}_{\mathbf{q}} \mathbf{u}_{\mathbf{q}}. \quad (\text{C1})$$

Here,  $\rho$  is the lattice mass density, the sans serif font denotes a matrix in Euclidean space, the first and second terms are the harmonic acoustic phonon Lagrangian  $\mathcal{L}_{ph}^{(0)}$ , and the third term comes from the phonon Hall viscosity and  $\mathbf{A}_{\mathbf{q}} = -\mathbf{A}_{\mathbf{q}}^T$ . For simplicity, we will ignore the anisotropy in  $\mathcal{L}_{ph}^{(0)}$  in the evaluation of the phonon Berry curvature.  $\mathbf{M}_{\mathbf{q}}$  for a 3D isotropic elastic medium is

$$\mathbf{M}_{\mathbf{q}} = \begin{pmatrix} c_1 q_x^2 + c_2 q^2 & c_1 q_x q_y & c_1 q_x q_z \\ c_1 q_x q_y & c_1 q_y^2 + c_2 q^2 & c_1 q_y q_z \\ c_1 q_x q_z & c_1 q_y q_z & c_1 q_z^2 + c_2 q^2 \end{pmatrix}. \quad (\text{C2})$$

Here  $c_{1,2}$  are the elastic modulus tensor coefficients. The eigenmodes include two degenerate transverse acoustic waves with sound wave velocity  $v_T = \sqrt{c_2/\rho}$ , and one longitudinal wave with  $v_L = \sqrt{(c_1 + c_2)/\rho}$ . However, the anisotropy of a crystal with lower symmetry breaks the degeneracy and mixes transverse and longitudinal waves at a generic momentum.

The antisymmetric  $\mathbf{A}$  matrices for  $\eta_{B_1 B_2}^H, \eta_{E_x E_y}^H$  (relevant when the field is along  $z$ -axis) are

$$\mathbf{A}_{\mathbf{q}}^{B_1 B_2} = \eta_{B_1 B_2}^H(\mathbf{q}) \begin{pmatrix} 0 & (q_x^2 + q_y^2) & 0 \\ -(q_x^2 + q_y^2) & 0 & 0 \\ 0 & 0 & 0 \end{pmatrix}, \quad \mathbf{A}_{\mathbf{q}}^{E_x E_y} = \eta_{E_x E_y}^H(\mathbf{q}) \begin{pmatrix} 0 & q_z^2 & q_y q_z \\ -q_z^2 & 0 & -q_x q_z \\ -q_y q_z & q_x q_z & 0 \end{pmatrix}, \quad (\text{C3})$$

where  $\eta_{\Gamma\Gamma'}^H(\mathbf{q})$  have been obtained in the main text. We reproduce the result here:  $\eta_{B_1 B_2}^H(\mathbf{q}) = \frac{\gamma_{B_1 B_2}}{(q_x^2 + q_y^2) + \delta_y^2}, \eta_{E_x E_y}^H(\mathbf{q}) = \frac{\gamma_{E_x E_y}}{(q_x^2 + q_y^2) + \delta_z^2}$ , where  $\delta_y = \Delta_y/v_m$ ,  $\delta_z = \sqrt{\Delta_z^2 + h^2}/v_m$ , and  $\gamma_{\Gamma\Gamma'} = \frac{h S^2 \lambda_{\Gamma} \lambda_{\Gamma'}}{v_m^3 g d_z a_0}$ .

## 1. Acoustic Faraday effect

The acoustic Faraday effect can be observed in an anisotropic medium only when the acoustic wave is propagating along a high symmetry direction, such that the transverse waves remain degenerate and do not mix with the longitudinal one. In our case, for a tetragonal lattice crystal with  $D_{4h}$  point group symmetry, there are indeed two degenerate transverse modes and one longitudinal mode at  $\mathbf{q} = q_z \hat{\mathbf{z}}$ , due to the  $C_{4z}$  symmetry in the little group of the high symmetry line. Upon applying a magnetic field along  $\hat{\mathbf{z}}$ , the magnetoelastic-coupling-induced phonon Hall viscosity in the  $\eta_{E_x E_y}^H$  channel lifts the degeneracy, and the left/right circularly polarized components are eigenmodes and non-degenerate.

To be specific, the Lagrangian of a wave with frequency  $\omega$  propagating along  $\hat{\mathbf{z}}$  with  $\mathbf{q} = q\hat{\mathbf{z}}$  can be expressed as:

$$\mathcal{L}_{ph}(q\hat{\mathbf{z}}) = \frac{1}{2} \mathbf{u}_{-q}^T \begin{pmatrix} \rho\omega^2 - c_2 q^2 & i2\eta_{E_x E_y}^H q^2 \omega \\ -i2\eta_{E_x E_y}^H q^2 \omega & \rho\omega^2 - c_2 q^2 \\ & & \rho\omega^2 - (c_1 + c_2)q^2 \end{pmatrix} \mathbf{u}_q. \quad (\text{C4})$$

While Eq. (C4) is obtained from Eq. (C1), which is only valid for an isotropic medium, it also describes the acoustic phonon along  $\hat{\mathbf{z}}$  for a tetragonal group. The transverse modes can be diagonalized as left ( $\hat{\mathbf{e}}_+ = \frac{1}{\sqrt{2}}\{1, i, 0\}^T$ ) and right ( $\hat{\mathbf{e}}_- = \frac{1}{\sqrt{2}}\{1, -i, 0\}^T$ ) circularly-polarized waves, with  $\rho\omega^2 - c_2 q_\pm^2 \mp 2\eta_{E_x E_y}^H q_\pm^2 \omega = 0$ . Consequently, the transverse linearly-polarized wave along  $\hat{\mathbf{z}}$  at frequency  $\omega_{ph}$  undergoes a Faraday rotation. The Faraday rotation angle per unit length, which is given by the difference of the left and right wave numbers,  $q_+$  and  $q_-$  respectively, is

$$\frac{\Phi}{L} = \frac{1}{2}(q_+ - q_-) = \frac{\omega_{ph}^2 \eta_{E_x E_y}^H(q\hat{\mathbf{z}})}{v_T^3 \rho} + O(\omega_{ph}^3), \quad (\text{C5})$$

where  $v_T = \sqrt{c_2/\rho}$  is the transverse sound wave velocity along  $\hat{\mathbf{z}}$ . Note that the magnon spectrum is dispersionless along  $q\hat{\mathbf{z}}$  due to the weak interlayer spin interactions, so  $\eta_{E_x E_y}^H(q\hat{\mathbf{z}}) = \frac{\gamma_{E_x E_y}}{\delta_z^2}$  from Eq. (8). This gives Eq. (9) in the main text.

## 2. Phonon thermal Hall conductivity

In this section, we show more details of the calculation of  $\kappa^H(T)$ . To compute the Berry curvature of the phonon bands, we first construct the effective phonon Hamiltonian  $H_{ph}^{\text{eff}}$  from the Legendre transformation of the Lagrangian  $\mathcal{L}_{ph}$ . The equation of motion for the pair of canonical variables  $\psi_{\mathbf{q}} = \{\mathbf{u}_{\mathbf{q}}, \mathbf{p}_{\mathbf{q}}\}^T$  can be obtained from  $\dot{\psi}_{\mathbf{q}} = -i[\psi_{\mathbf{q}}, H_{ph}^{\text{eff}}]$  ( $\hbar = 1$ ). This gives the band Hamiltonian  $\mathcal{H}_{\mathbf{q}}$  in the basis of  $\psi_{\mathbf{q}}$ . The phonon band energies/eigenstates can then be computed as eigenvalues/eigenvectors of  $\mathcal{H}_{\mathbf{q}}$ .

To be specific, we find

$$H_{ph}^{\text{eff}} = \sum_{\mathbf{q}} \frac{(\mathbf{p}_{-\mathbf{q}} - \mathbf{A}_{-\mathbf{q}})(\mathbf{p}_{\mathbf{q}} - \mathbf{A}_{\mathbf{q}})}{2\rho} + \frac{1}{2} \mathbf{u}_{-\mathbf{q}}^T \mathbf{M}_{\mathbf{q}} \mathbf{u}_{\mathbf{q}} \quad (\text{C6})$$

where the canonical momentum is defined as  $\mathbf{p}_{\mathbf{q}} = \frac{\partial \mathcal{L}_{ph}}{\partial \dot{\mathbf{u}}_{-\mathbf{q}}} = \rho \dot{\mathbf{u}}_{\mathbf{q}} + \mathbf{A}_{\mathbf{q}} \mathbf{u}_{\mathbf{q}} = \rho \dot{\mathbf{u}}_{\mathbf{q}} + \mathbf{A}_{\mathbf{q}}$ . We then obtain the equation of motion in matrix form as  $\dot{\psi}_{\mathbf{q}} = -i\mathcal{H}_{\mathbf{q}}\psi_{\mathbf{q}}$ , where

$$\mathcal{H}_{\mathbf{q}} = \frac{i}{\rho} \begin{pmatrix} -\mathbf{A}_{\mathbf{q}} & \mathbb{I} \\ -\rho \mathbf{M}_{\mathbf{q}} & -\mathbf{A}_{\mathbf{q}} \end{pmatrix}. \quad (\text{C7})$$

Defining  $\xi_{\mathbf{q},\sigma}^{L(R)}$  as the left/right eigenvector of  $\mathcal{H}_{\mathbf{q}}$  for the phonon branch  $\sigma$  with eigenvalue/spectrum  $\omega_{\mathbf{q},\sigma}$ , the Berry curvature is

$$\Omega_{\mathbf{q},\sigma}^i = -\text{Im} [\epsilon_{ijk} \partial_{q_j} \xi_{\mathbf{q},\sigma}^L \partial_{q_k} \xi_{\mathbf{q},\sigma}^R]. \quad (\text{C8})$$

As  $\mathcal{H}_{\mathbf{q}}$  is not Hermitian,  $\xi_{\mathbf{q},\sigma}^{L(R)}$  are not Hermitian conjugate with each other, and they are normalized with  $\xi_{\mathbf{q},\sigma'}^L \xi_{\mathbf{q},\sigma}^R = \delta_{\sigma\sigma'}$ .

The relation between the phonon Berry curvature and the intrinsic thermal Hall conductivity has been obtained in Ref. [10].  $\kappa_{jk}^{\text{ph}}$  in terms of  $\Omega_{\mathbf{q},\sigma}^i$  and  $\omega_{\mathbf{q},\sigma}$  is

$$\frac{\kappa_{jk}^{\text{ph}}}{T} = -\frac{1}{T^2} \int_0^\infty dE E^2 \sigma_{jk}(E) \frac{dn_B^{\text{eq}}(E)}{dE} = \int_0^\infty dx x^2 \frac{e^x}{(e^x - 1)^2} \sigma_{jk}(xT) \quad (\text{C9})$$

where

$$\sigma_{jk}(E) = -\sum_\sigma \int \frac{d^3q}{(2\pi)^3} \epsilon_{ijk} \Omega_{\mathbf{q},\sigma}^i \Theta(E - \omega_{\mathbf{q},\sigma}) = -\frac{1}{4\pi^2} \int_0^\epsilon dE' E'^2 \sum_\sigma \int \frac{d\phi_{\mathbf{q}}}{2\pi} d\theta_{\mathbf{q}} \sin \theta_{\mathbf{q}} \frac{1}{v_\sigma^3} \Omega_{\mathbf{q},\sigma}^i \Theta(E - E'). \quad (\text{C10})$$

$n_B^{\text{eq}}(E) = 1/(e^{\beta E} - 1)$  is the equilibrium Bose distribution function.  $\sum_\sigma$  sums over all eigenstates with positive energy.  $\theta_{\mathbf{q}}, \phi_{\mathbf{q}}$  are the polar coordinates for  $\mathbf{q}$ , defined through  $\mathbf{q} = \{q \sin \theta_{\mathbf{q}} \cos \phi_{\mathbf{q}}, q \sin \theta_{\mathbf{q}} \sin \phi_{\mathbf{q}}, q \cos \theta_{\mathbf{q}}\}$ .

Importantly, the behavior of  $\kappa^H/T$  v.s. temperature is determined by the functional form of  $\sigma_{jk}(E)$  as we analyze below. As an example, we compute  $\kappa_{xy}^H(T)/T$  when the field is  $\mathbf{h} = h\hat{z}$  perturbatively in the Hall viscosity coefficient, keeping the first order in  $\eta^H$ . The antisymmetric  $\mathbf{A}$  matrices for  $\eta_{B_1 B_2}^H, \eta_{E_x E_y}^H$  are presented in Eq. (C3).

To linear order in  $\eta^H$ , the contributions from different Hall viscosity terms simply add up. We find the Berry curvature  $\Omega_{\mathbf{q},\sigma}^{z,\Gamma\Gamma'}$  from  $\eta_{\Gamma\Gamma'}^H$  of the two degenerate transverse phonon bands  $\sigma = T_1, T_2$  and one longitudinal phonon band  $\sigma = L$  as

$$\begin{aligned} \Omega_{\mathbf{q},T_1}^{z,B_1 B_2} + \Omega_{\mathbf{q},T_2}^{z,B_1 B_2} &= \frac{\gamma_{B_1 B_2} v_T^2 \sin^2 \theta_{\mathbf{q}} (v_L^2 + 3v_T^2) [-4 \cos 2\theta_{\mathbf{q}} (3\delta_y^2 v_T^2 + (v_T q)^2) - 20\delta_y^2 v_T^2 + 3(v_T q)^2 \cos 4\theta_{\mathbf{q}} + (v_T q)^2]}{2\rho q v_T (v_T - v_L)(v_L + v_T) (2\delta_y^2 v_L^2 - (v_T q)^2 \cos 2\theta_{\mathbf{q}} + (v_T q)^2)^2} \\ \Omega_{\mathbf{q},L}^{z,B_1 B_2} &= \frac{\gamma_{B_1 B_2} v_L^2 \sin^2 \theta_{\mathbf{q}} (3v_L^2 + v_T^2) [-4 \cos 2\theta_{\mathbf{q}} (3\delta_y^2 v_L^2 + (v_L q)^2) - 20\delta_y^2 v_L^2 + 3(v_L q)^2 \cos 4\theta_{\mathbf{q}} + (v_L q)^2]}{2\rho v_L q (v_L - v_T)(v_L + v_T) (2\delta_y^2 v_L^2 - (v_L q)^2 \cos 2\theta_{\mathbf{q}} + (v_L q)^2)^2} \\ \Omega_{\mathbf{q},T_1}^{z,E_x E_y} + \Omega_{\mathbf{q},T_2}^{z,E_x E_y} &= \frac{\gamma_{E_x E_y} v_T^2 \cos^2 \theta_{\mathbf{q}} (v_L^2 + 3v_T^2) [-12 \cos 2\theta_{\mathbf{q}} (\delta_z^2 v_T^2 + (v_T q)^2) - 4\delta_z^2 v_T^2 + 3(v_T q)^2 \cos 4\theta_{\mathbf{q}} + 9(v_T q)^2]}{\rho v_T q (v_T - v_L)(v_L + v_T) (2\delta_z^2 v_T^2 - (v_T q)^2 \cos 2\theta_{\mathbf{q}} + (v_T q)^2)^2} \\ \Omega_{\mathbf{q},L}^{z,E_x E_y} &= \frac{\gamma_{E_x E_y} v_L^2 \cos^2 \theta_{\mathbf{q}} (3v_L^2 + v_T^2) [-12 \cos 2\theta_{\mathbf{q}} (\delta_z^2 v_L^2 + (v_L q)^2) - 4\delta_z^2 v_L^2 + 3(v_L q)^2 \cos 4\theta_{\mathbf{q}} + 9(v_L q)^2]}{\rho v_L q (v_L - v_T)(v_L + v_T) (2\delta_z^2 v_L^2 - (v_L q)^2 \cos 2\theta_{\mathbf{q}} + (v_L q)^2)^2}, \end{aligned} \quad (\text{C11})$$

where  $q = |\mathbf{q}|$ . From Eqs. (C11) and (C10), we find

$$\begin{aligned} \sigma_{xy}^{B_1 B_2}(v_{\text{ph}} \delta_y t) &= -\frac{4\gamma_{B_1 B_2}}{v_{\text{ph}} \rho} \left( -\frac{1}{1+t^2} - \frac{(3+4t^2) \log(\sqrt{1+t^2}+t)}{t^3(1+t^2)^{3/2}} + \frac{3}{t^2} \right) = -\frac{4\gamma_{B_1 B_2}}{v_{\text{ph}} \rho} f_y(t) \\ \sigma_{xy}^{E_x E_y}(v_{\text{ph}} \delta_z t) &= -\frac{8\gamma_{E_x E_y}}{v_{\text{ph}} \rho} \left( \frac{(3+2t^2) \log(\sqrt{1+t^2}+t)}{t^3(1+t^2)^{3/2}} - \frac{3}{t^2} \right) = -\frac{8\gamma_{E_x E_y}}{v_{\text{ph}} \rho} f_z(t). \end{aligned} \quad (\text{C12})$$

Corrections at order  $(v_L - v_T)/v_L$  are subleading and nonsingular, and so they are ignored in the above expressions.  $v_{\text{ph}}$  denotes the averaged sound velocity. Note that  $\sigma_{xy}^{\Gamma\Gamma'}(E)$  is only a function of  $t = E/(v_{\text{ph}} \delta_\alpha(\Gamma\Gamma'))$ , where  $\alpha(B_1, B_2) = y, \alpha(E_x, E_y) = z$ . For both  $\sigma_{xy}^{B_1 B_2}, \sigma_{xy}^{E_x E_y}$ , the function in the parentheses, defined as  $f_{y,z}(t)$ , increases as  $\sim t^2$  for  $t \ll 1$ , and decreases to zero as  $\sim \frac{1}{t^2}$  for  $f_y(t)$ , and as  $\sim \frac{\ln t}{t^2}$  for  $f_z(t)$  at  $t \gg 1$  (see Fig. 3).

From Eq. (C9) and (C12), defining a dimensionless temperature  $\tilde{T} = T/(v_{\text{ph}} \delta_\alpha)$ ,

$$\frac{\kappa_{xy}^{\Gamma\Gamma'}}{T} \sim F_{\alpha(\Gamma\Gamma')}(\tilde{T}), \quad F_{\alpha(\Gamma\Gamma')}(\tilde{T}) = \int_0^\infty dx x^2 \frac{e^x}{(e^x - 1)^2} f_\alpha(x\tilde{T}). \quad (\text{C13})$$

It is straightforward to see that the behavior of  $\kappa^H/T$  is only a function of  $\tilde{T} = T/(v_{\text{ph}} \delta_\alpha)$ . Also, noting that the Boltzmann distribution decays exponentially at high temperature,  $\frac{\kappa_{xy}^{\Gamma\Gamma'}}{T}$  at  $\tilde{T} \ll 1 (T \ll v_{\text{ph}} \delta_\alpha)$  and  $\tilde{T} \gg 1 (T \gg v_{\text{ph}} \delta_\alpha)$  may be inferred from  $f_\alpha(t)$  analytically. When  $\tilde{T} \ll 1$ , it mainly comes from  $f_\alpha(t) \sim t^2$  at  $t \ll 1$ , so we have  $\frac{\kappa_{xy}^{\Gamma\Gamma'}}{T} \sim T^2$ . When  $\tilde{T} \gg 1$ , the scaling of  $\frac{\kappa_{xy}^{\Gamma\Gamma'}}{T}$  is more complicated as it depends on  $f_\alpha(t)$  in the whole range. From the decaying behavior of  $f_\alpha(t)$  when  $t \gtrsim 1$ , we find that  $\frac{\kappa_{xy}^{\Gamma\Gamma'}}{T} \sim 1/T^\zeta$  at  $T \gg v_{\text{ph}} \delta_\alpha$ , with  $\zeta \sim 1$  up to a logarithmic factor. In the intermediate regime,  $\frac{\kappa_{xy}^{\Gamma\Gamma'}}{T}$  can be fit to an exponential empirically as  $e^{-T/T_0^{\Gamma\Gamma'}} + \text{constant}$ . From the numerical fit, we find  $T_0^{B_1 B_2} \sim 2.3 v_{\text{ph}} \delta_y, T_0^{E_x E_y} \sim 3.3 v_{\text{ph}} \delta_z$ .

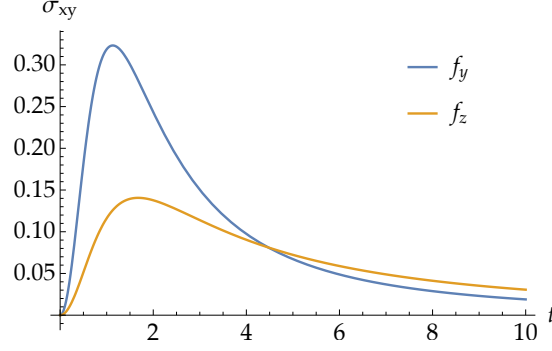


FIG. 3. Behavior of  $f_{y,z}(t)$  defined in Eq. (C12).

#### D: Contribution to $\eta^H$ from four-point correlation functions

In this section, we discuss contributions to  $\eta^H$  from four-point correlation functions of the spin fields. We argue that contributions at this order are subleading at low temperature, and can thus be ignored.

We consider the contribution to  $\eta_{B_1 B_2}^H$  ( $\eta_{E_x E_y}^H$  is similar). From Eq. (3) and Tab. III, we find

$$\begin{aligned} & \langle \mathcal{O}_{B_1}(-\mathbf{q}, \tau) \mathcal{O}_{B_2}(\mathbf{q}, 0) \rangle_{\omega_n} \\ & \sim \frac{1}{L^2} \sum_{\mathbf{k}, \mathbf{k}'} (\varsigma_1 \langle n_{y, -\mathbf{k} - \mathbf{q}_\perp}(\tau) n_{y, \mathbf{k}}(\tau) n_{y, \mathbf{k}' + \mathbf{q}_\perp}(0) m_{z, -\mathbf{k}'}(0) \rangle_{\omega_n} + \varsigma_2 \langle n_{z, -\mathbf{k} - \mathbf{q}_\perp}(\tau) n_{z, \mathbf{k}}(\tau) n_{z, \mathbf{k}' + \mathbf{q}_\perp}(0) m_{y, -\mathbf{k}'}(0) \rangle_{\omega_n}) \\ & \sim T \frac{1}{L^2} \sum_{\mathbf{k}, m} (\varsigma_1 \langle n_{y, -\mathbf{k} - \mathbf{q}_\perp} m_{z, \mathbf{k} + \mathbf{q}_\perp} \rangle_{\omega_m} \langle n_{y, \mathbf{k}}(\tau) n_{y, -\mathbf{k}} \rangle_{-\omega_m + \omega_n} + \varsigma_2 \langle n_{z, -\mathbf{k} - \mathbf{q}_\perp} m_{y, \mathbf{k} + \mathbf{q}_\perp} \rangle_{\omega_m} \langle n_{z, \mathbf{k}}(\tau) n_{z, -\mathbf{k}} \rangle_{-\omega_m + \omega_n}). \quad (\text{D1}) \end{aligned}$$

where  $\varsigma_1, \varsigma_2$  are dimensionless coefficients that determine the magnitude and sign of the two types of four-point correlations. Following the analysis in Sec. A 1, an overall factor  $\frac{\lambda_\Gamma \lambda_{\Gamma'}}{d_z} \left( \frac{S^2}{a_0^2} \right)^2 \chi h$  is absorbed into  $\sim$ .

For simplicity, we consider the limit when  $q = |\mathbf{q}| \rightarrow 0$ . After summing over the Matsubara frequencies  $\omega_m$  and analytical continuing to real frequencies,  $\eta_{B_1 B_2}^H$  from Eq. (D1) can be expressed as

$$\begin{aligned} [\eta_{B_1, B_2}^H(\mathbf{q})]^{(2)} & \sim \frac{\lambda_\Gamma \lambda_{\Gamma'}}{d_z} \left( \frac{S^2}{a_0^2} \right)^2 \chi h \frac{a_0^2}{S} v_m g a_0 \\ & \quad \frac{1}{a_0^2} \frac{1}{N_x N_y} \sum_{\mathbf{k}} \left\{ \frac{\varsigma_1}{(\omega_{y, \mathbf{k}} + \omega_{y, \mathbf{k} - \mathbf{q}_\perp})^2} \left( \frac{1}{\omega_{y, \mathbf{k}}} \coth \frac{\beta \omega_{y, \mathbf{k}}}{2} + \frac{1}{\omega_{y, \mathbf{k} - \mathbf{q}_\perp}} \coth \frac{\beta \omega_{y, \mathbf{k} - \mathbf{q}_\perp}}{2} \right) \right. \\ & \quad \left. - \frac{\varsigma_2}{(\omega_{z, \mathbf{k}} + \omega_{z, \mathbf{k} - \mathbf{q}_\perp})^2} \left( \frac{1}{\omega_{z, \mathbf{k}}} \coth \frac{\beta \omega_{z, \mathbf{k}}}{2} + \frac{1}{\omega_{z, \mathbf{k} - \mathbf{q}_\perp}} \coth \frac{\beta \omega_{z, \mathbf{k} - \mathbf{q}_\perp}}{2} \right) \right\} \\ & \xrightarrow{q \rightarrow 0} \gamma_{B_1 B_2} v_m^3 g a_0 \frac{1}{a_0^2} \int_{-\frac{\pi}{a_0}}^{\frac{\pi}{a_0}} \int_{-\frac{\pi}{a_0}}^{\frac{\pi}{a_0}} \frac{d^2 k}{(2\pi/a_0)^2} \left\{ \frac{\varsigma_1}{\omega_{y, \mathbf{k}}^3} \coth \frac{\beta \omega_{y, \mathbf{k}}}{2} - \frac{\varsigma_2}{\omega_{z, \mathbf{k}}^3} \coth \frac{\beta \omega_{z, \mathbf{k}}}{2} \right\} \\ & \sim \gamma_{B_1 B_2} v_m^3 g a_0 \frac{1}{T v_m^2} \left[ \varsigma_1 \mathcal{F} \left( \frac{v_m \delta_y}{2T} \right) - \varsigma_2 \mathcal{F} \left( \frac{v_m \delta_z}{2T} \right) \right] \\ & \sim \gamma_{B_1 B_2} v_m g a_0 \begin{cases} \frac{1}{v_m \delta_y} & T \ll v_m \delta_y \\ \frac{T}{(v_m \delta_y)^2} & T \gg v_m \delta_y \end{cases} \quad (\text{D2}) \end{aligned}$$

where  $\mathcal{F}(x) = \int_x^\infty dz \frac{1}{z^2} \coth z$ , and  $\delta_y \ll \delta_z$  has been applied to obtain the last line. As our interest here is the relative strength of four-point contribution compared to two-point contribution, numerical coefficients are subsumed in the “ $\sim$ ”. The superscript “(2)” denotes that it is a second order contribution. Note that the contribution from 2 magnons is much smaller than that from 1 magnon by a factor  $\frac{gT}{v_m a_0^{-1}} \sim \frac{T}{JS^2} \ll 1$ . For this reason, only contributions from 1 magnon terms are considered further in the main text.

### E: Microscopic Hamiltonian

In this section, we present the microscopic spin Hamiltonian and spin-lattice coupling Hamiltonian. The microscopic analysis is helpful to infer the spin gap and relevant spin-lattice coupling in the low energy effective action derived in the main text from a symmetry analysis.

The microscopic Hamiltonian must be invariant under the grey magnetic space group  $\mathbf{G}$  (see Table I) of the crystal. It is useful to decompose the part involving the spin as:

$$\begin{aligned} H &= H_s + H_{sl} \\ &= H_s^{(0)} + \lambda_{SOC} H_s^{(1)} + H_{sl}^{(0)} + \lambda_{SOC} H_{sl}^{(1)}, \end{aligned} \quad (E1)$$

where  $s$  refers to “spin” and  $sl$  to “spin-lattice coupling”. We assume weak SOC (as e.g. appropriate for cuprates), and accordingly separate terms of 0th order in SOC ( $H_s^{(0)} + H_{sl}^{(0)}$ ) and those that require SOC ( $H_s^{(1)} + H_{sl}^{(1)}$ ). This is defined by symmetry:  $H_s^{(0)} + H_{sl}^{(0)}$  also has a global  $SO(3)$  spin-rotation symmetry, so is also invariant under  $SO(3)_s$ , while  $H_s^{(1)} + H_{sl}^{(1)}$  must break  $SO(3)_s$ .

$H_s$  – The spin Hamiltonian reads

$$\begin{aligned} H_s^{(0)} &= \sum_i J(\mathbf{S}_i \cdot \mathbf{S}_{i+\hat{x}} + \mathbf{S}_i \cdot \mathbf{S}_{i+\hat{y}}) \\ H_s^{(1)} &= \sum_{\mathbf{r}} J'_1 (S_{\mathbf{r}}^x S_{\mathbf{r}+\hat{x}}^x - S_{\mathbf{r}}^y S_{\mathbf{r}+\hat{x}}^y - S_{\mathbf{r}}^x S_{\mathbf{r}+\hat{y}}^x + S_{\mathbf{r}}^y S_{\mathbf{r}+\hat{y}}^y) + J'_z (S_{\mathbf{r}}^z S_{\mathbf{r}+\hat{x}}^z + S_{\mathbf{r}}^z S_{\mathbf{r}+\hat{y}}^z) \\ &\quad + J'_2 (S_{\mathbf{r}}^x S_{\mathbf{r}+\hat{a}}^y + S_{\mathbf{r}}^y S_{\mathbf{r}+\hat{a}}^x - S_{\mathbf{r}}^x S_{\mathbf{r}+\hat{b}}^y - S_{\mathbf{r}}^y S_{\mathbf{r}+\hat{b}}^x) \end{aligned} \quad (E2)$$

where, as before,  $\hat{\mathbf{a}}, \hat{\mathbf{b}} = \frac{1}{\sqrt{2}}(\pm\hat{x} + \hat{y})$  are second neighbor vectors. The nearest neighbor exchange dominates and  $J \sim 0.1$  eV. From Refs. [25, 26], the anisotropy gap  $\Delta_{y,z}$  can be estimated for  $\text{Sr}_2\text{CuO}_2\text{Cl}_2$  from the spin exchange interactions that require SOC. The XXZ anisotropic exchange  $J'_z$  is positive, which stabilizes the staggered order in the  $xy$  plane.  $J'_z$  introduces a gap for out-of-plane fluctuations  $\Delta_z = 4SJ'_z \sim 3$  meV, where the factor of 4 comes from the coordination number of square lattice. While  $J'_{1,2} \ll J$ ,  $J'_1$  is still important to introduce an *effective* mass gap to the in-plane Goldstone mode at order  $1/S$ . In Ref. [25], by studying the dependence of the quantum zero point energy on the angle  $\phi$  of the Néel order relative to  $\hat{x}$ , it is shown that  $J'_1$  stabilize Néel order with  $\phi = \pi/4 \bmod \pi/2$ , and thus the in-plane Goldstone mode acquires an effective gap, which is estimated to be  $\Delta_y = 0.05$  meV when  $S = 1/2$ .

$H_{sl}$  – In this work, we assume the spin-lattice coupling comes from the modification to the exchange coupling when the direction and length of the bond change due to an elastic deformation. The microscopic spin-lattice Hamiltonian can be obtained by finding all the terms composed of  $\mathcal{E}_\Gamma$  and  $\mathcal{O}_\Gamma$  invariant under  $\mathbf{G}$ , where  $\mathcal{E}_\Gamma$  is the strain tensor decomposed into irreps of  $D_{4h}$  (see Eq. (6) in the main text), and on the lattice we take  $\mathcal{O}_\Gamma$  to be composed of bilinears of spin operators on nearby sites, chosen to transform under  $D_{4h}$  with the same irrep  $\Gamma$ . In real space, we find

$$\begin{aligned} H_{sl}^{(0)} &= \lambda_{A_1} \sum_{\mathbf{r}} (\mathcal{E}_{A_1})_{\mathbf{r}} (\mathbf{S}_{\mathbf{r}} \cdot \mathbf{S}_{\mathbf{r}+\hat{x}} + \mathbf{S}_{\mathbf{r}} \cdot \mathbf{S}_{\mathbf{r}+\hat{y}}) + \frac{\lambda_{B_1}}{2} \sum_{\mathbf{r}} (\mathcal{E}_{B_1})_{\mathbf{r}} (\mathbf{S}_{\mathbf{r}} \cdot \mathbf{S}_{\mathbf{r}+\hat{x}} - \mathbf{S}_{\mathbf{r}} \cdot \mathbf{S}_{\mathbf{r}+\hat{y}}) + \\ &\quad \frac{\lambda_{B_2}}{2} \sum_{\mathbf{r}} (\mathcal{E}_{B_2})_{\mathbf{r}} (\mathbf{S}_{\mathbf{r}} \cdot \mathbf{S}_{\mathbf{r}+\hat{a}} - \mathbf{S}_{\mathbf{r}} \cdot \mathbf{S}_{\mathbf{r}+\hat{b}}). \end{aligned} \quad (E3)$$

Here we denote by  $(\mathcal{E}_\Gamma)_{\mathbf{x}}$  the strain at position  $\mathbf{x}$  – note that since the strain is slowly varying, shifts of this coordinate by order one displacements do not modify the results. The XXZ anisotropy may be ignored here *in the spin-lattice coupling* as it is negligibly small and not essential (it is, however, important in the spin Hamiltonian itself). The anisotropic spin-lattice coupling terms, keeping spin operators on the nearest possible pairs of spins in each channel, give  $H_{sl}^{(1)}$  in the form

$$\begin{aligned} H_{sl}^{(1)} &= \frac{\lambda'_{B_1}}{2} \sum_{\mathbf{r}} (\mathcal{E}_{B_1})_{\mathbf{r}} \left( S_{\mathbf{r}}^x S_{\mathbf{r}+\hat{x}}^x - S_{\mathbf{r}}^y S_{\mathbf{r}+\hat{x}}^y + S_{\mathbf{r}}^x S_{\mathbf{r}+\hat{y}}^x - S_{\mathbf{r}}^y S_{\mathbf{r}+\hat{y}}^y \right) + \\ &\quad \frac{\lambda'_{B_2}}{2} \sum_{\mathbf{r}} (\mathcal{E}_{B_2})_{\mathbf{r}} \left( S_{\mathbf{r}}^x S_{\mathbf{r}+\hat{a}}^y + S_{\mathbf{r}}^y S_{\mathbf{r}+\hat{a}}^x + S_{\mathbf{r}}^x S_{\mathbf{r}+\hat{b}}^y + S_{\mathbf{r}}^y S_{\mathbf{r}+\hat{b}}^x \right) + \\ &\quad \frac{\lambda'_E}{2} \sum_{\mathbf{r}} (\mathcal{E}_E)_{\mathbf{r}} \left[ (1+\beta) (S_{\mathbf{r}}^x S_{\mathbf{r}+\hat{x}}^z + S_{\mathbf{r}}^z S_{\mathbf{r}+\hat{x}}^x) + (1-\beta) (S_{\mathbf{r}}^x S_{\mathbf{r}+\hat{y}}^z + S_{\mathbf{r}}^z S_{\mathbf{r}+\hat{y}}^x) \right] + \end{aligned}$$

$$\frac{\lambda'_E}{2} \sum_{\mathbf{r}} (\mathcal{E}_{E_y})_{\mathbf{r}} \left[ (1 - \beta) (S_{\mathbf{r}}^y S_{\mathbf{r} \pm \hat{x}}^z + S_{\mathbf{r}}^z S_{\mathbf{r} \pm \hat{x}}^y) + (1 + \beta) (S_{\mathbf{r}}^y S_{\mathbf{r} \pm \hat{y}}^z + S_{\mathbf{r}}^z S_{\mathbf{r} \pm \hat{y}}^y) \right]. \quad (\text{E4})$$

Note that in the  $\Gamma = E$  channel, there are two symmetry allowed spin-lattice coupling terms, of strength  $\lambda'_E$  and  $\beta\lambda'_E$ , where  $\beta$  is a dimensionless parameter defined by Eq. (E4).

The above microscopic spin-lattice couplings give rise to continuum spin-lattice couplings of the form in Eq. (2) of the main text by taking a continuum limit. In particular, one uses the NLSM decomposition with  $\mathbf{S}_{\mathbf{r}} = S\mathbf{e}_{\mathbf{r}}$  with  $\mathbf{e}_{\mathbf{r}}$  in Eq. (A1), and expresses the Hamiltonian thereby in terms of  $\mathbf{n}$  and  $\mathbf{m}$ , which are presumed to be slowly varying functions of position. To zeroth order in the gradient expansion of these fields, derivatives  $\partial_{\mu}\mathbf{n}, \partial_{\mu}\mathbf{m}$  are neglected. The result then takes the *schematic* form

$$H_{\text{sl}}^{(\text{loc})} \sim \sum_z \frac{1}{a_0^2} \int d\mathbf{x} d\mathbf{y} [\lambda_{A_1} \mathcal{E}_{A_1} \mathbf{s} \cdot \mathbf{s} + \lambda'_{B_1} \mathcal{E}_{B_1} (s^x s^x - s^y s^y) + \lambda'_{B_2} \mathcal{E}_{B_2} (s^x s^y + s^y s^x) + \lambda'_{E_x} \mathcal{E}_{E_x} (s^x s^z + s^z s^x) + \lambda'_{E_y} \mathcal{E}_{E_y} (s^y s^z + s^z s^y)]. \quad (\text{E5})$$

Here each term represents a sum of two contributions, one with  $\mathbf{s} = S\mathbf{m}$ , and another with  $\mathbf{s} = S\mathbf{n}$ , and some sign differences may appear between these terms. Here, we summed over 2d magnetic layers ( $\sum_z$ ), where the layer index is  $z$ . In the limit of decoupled magnetic layers, we considered the continuous limit as  $\sum_{\mathbf{r}} \rightarrow \sum_z \frac{1}{a_0^2} \int d\mathbf{x} d\mathbf{y}$  (see the discussion of Eq. (A7) for more details). From Eq. (E5), we see that  $H_{\text{sl}}$  in all channels  $\Gamma \neq A_1$  requires breaking  $SO(3)_s$ , and thus requires SOC microscopically. Eq. (E5) give results consistent with the general symmetry analysis in terms of continuous spin fields  $\mathbf{n}$  and  $\mathbf{m}$  (c.f. Table III).

### F: Phonon Hall viscosity for in-plane magnetic field

For completeness, we have also analyzed the phonon Hall viscosity for in-plane magnetic fields. For concreteness, the field is applied along the  $y$ -axis. Such a scenario can be relevant to the phonon Hall effect when the heat current is applied perpendicular to the  $\text{CuO}_2$  planes, i.e. upon studying  $\kappa_{xz}$ . The analysis follows that for the out-of-plane field presented in the main text. Here, we summarize the main results.

The magnetic space group for a paramagnet and AFM with staggered order in the  $xy$  plane at an arbitrary  $\phi \neq 0 \bmod \pi/4$  and  $\phi = 0$  relative to  $\hat{x}$ , when the field is along  $\hat{y}$ , is summarized in Table V.

	zero field	$\mathbf{h} = h\hat{y}$	
		lattice and spin	lattice effective
paramagnet	$G = P4/mmm1'$	$G(\mathbf{0}, h\hat{y}) = \langle X, Y, C_{2y}, i, \mathcal{TC}_{2z} \rangle$	$G^{\text{eff}}(\mathbf{0}, h\hat{y}) = \langle C_{2y}, i, \mathcal{TC}_{2z} \rangle$
high sym. AFM	$G(\hat{x}, \mathbf{0}) = \langle i, \mathcal{TX}, \mathcal{TY}, C_{2x}, \mathcal{TC}_{2z} \rangle$	$G(\hat{x}, h\hat{y}) = \langle i, XY, \mathcal{TC}_{2z} \rangle$	$G^{\text{eff}}(\hat{x}, h\hat{y}) = \langle i, \mathcal{TC}_{2z} \rangle$
low sym. AFM	$G(\hat{e}, \mathbf{0}) = \langle i, \mathcal{TX}, \mathcal{TY}, \mathcal{TC}_{2z} \rangle$	$G(\hat{e}, h\hat{y}) = \langle i, XY, \mathcal{TC}_{2z} \rangle$	$G^{\text{eff}}(\hat{e}, h\hat{y}) = \langle i, \mathcal{TC}_{2z} \rangle$

TABLE V. Summary of the magnetic space group (in the Hermann-Mauguin notation) for layer group  $G = P4/mmm$  with  $\mathbf{h} = h\hat{y}$ . Same to Tab. I in the main text, rows denote different values for  $\mathbf{n}$ : without magnetic order, and for the two distinct orientations of the staggered magnetization in the  $xy$  plane (here  $\hat{e}$  is a generic vector *not* along a high-symmetry axis in the plane), and columns specify the zero and finite field cases, and the effective magnetic group for the effective lattice theory. The symbol  $\langle \cdot \rangle$  indicates the group generated by the “.” operations.

Note that  $\eta_{E_x E_y}^H = 0$  due to the  $\mathcal{TC}_{2z}$  symmetry, so there is no AFE. To generate a nonzero phonon Berry curvature  $\Omega^y$ , both time-reversal and mirror symmetries perpendicular to the  $xz$  plane ( $\sigma_h$  and  $\sigma_{vx}$  in the  $D_{4h}$  group) should be broken. The symmetry-allowed Hall viscosity that generates a nonzero phonon Berry curvature reads

$$\mathcal{S}_{\text{PHV}, h\hat{y}} = \int d^3x d\tau \{ \eta_{A_1 E_x}^H (\mathcal{E}_{A_1} \dot{\mathcal{E}}_{E_x} - \dot{\mathcal{E}}_{A_1} \mathcal{E}_{E_x}) + \eta_{B_1 E_x}^H (\mathcal{E}_{B_1} \dot{\mathcal{E}}_{E_x} - \dot{\mathcal{E}}_{B_1} \mathcal{E}_{E_x}) + \eta_{B_2 E_y}^H (\mathcal{E}_{B_2} \dot{\mathcal{E}}_{E_y} - \dot{\mathcal{E}}_{B_2} \mathcal{E}_{E_y}) \}. \quad (\text{F1})$$

To obtain the Hall viscosity induced by spin-lattice coupling, we find  $\mathcal{O}_{\Gamma}(\mathbf{x}, \tau)$  (see Eq. (2)) in terms of the spin fields as tabulated in Table VI.

At leading order in  $1/S$ , this gives

$$\eta_{A_1, E_x}^H \sim h \langle m_y n_z \rangle, \quad \eta_{B_1, E_x}^H \sim h \langle m_y n_z \rangle, \quad \eta_{B_2, E_y}^H \sim h \langle m_z n_y \rangle. \quad (\text{F2})$$



	$\epsilon n$	$\epsilon nn$	$\epsilon mm$	$\epsilon nmm$
$\mathcal{O}_{A_1}$		$n_y n_y, n_z n_z$	$\hbar m_y$	
$\mathcal{O}_{B_1}$		$n_y n_y, n_z n_z$	$\hbar m_y$	
$\mathcal{O}_{B_2}$	$n_y$		$-\hbar n_y m_y$	$\hbar n_y m_y, \hbar n_z m_z$
$\mathcal{O}_{E_x}$	$n_z$		$-\hbar n_y m_z$	$\hbar n_z m_y, \hbar n_y m_z$
$\mathcal{O}_{E_y}$		$n_y n_z$	$\hbar m_z$	

TABLE VI. Magnetic operators in the high symmetry AFM in the presence of a small field along the  $y$ -axis. Other factors, e.g.  $S^2, \chi, 1/a_0^2, n_0$ , have been omitted in the table.

Note that at leading order in  $1/S$ , the Hall viscosity coefficients are determined by the same sets of spin correlators as when  $\mathbf{h} = h\hat{\mathbf{z}}$ . However, this is restricted to when the in-plane field is perpendicular to the staggered order. If the external field also has components parallel to the staggered order, we find that  $\langle n_y n_z \rangle_\omega \sim i\hbar\omega$  also contribute to a nonzero Hall viscosity.